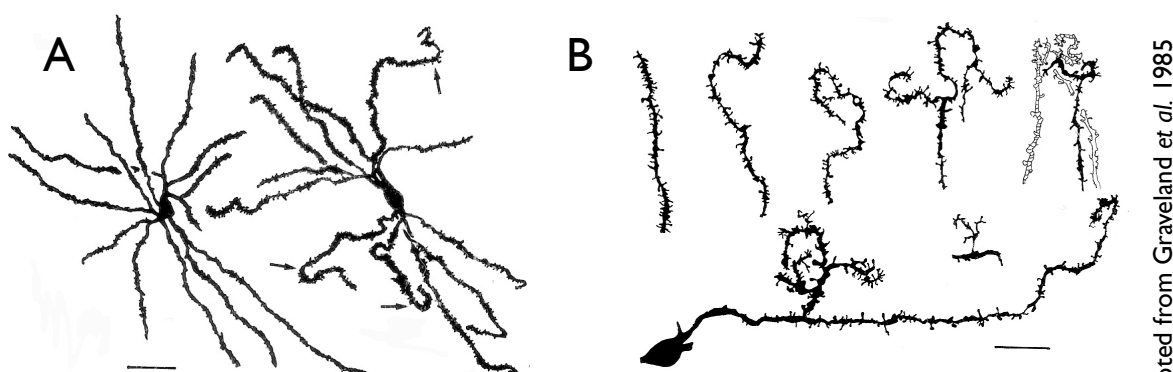


## Chapter 6.

### *Golgi Studies*

The landmark study using the Golgi impregnation technique carried out by DiFiglia and colleagues (Graveland *et al.* 1985) on human *postmortem* tissue revealed many new aspects of the HD pathology. The study found that there were many pathological differences found in the medium spiny neurons of the *striatum*, thought to be most affected in the disease.



**Figure 6.1:** Drawing showing a control neuron on the left and the HD neuron can be seen on the right with several marked differences; firstly the dendrites are hyper-spiny and there are hooks seen at the distal ends (A), the scale bar represents 50  $\mu\text{m}$ . To the far right are examples of contorted growths (B), the scale bar represents 25  $\mu\text{m}$ .

A handful of other studies have described structural changes and in particular changes in the dendritic structure of several types of neuron vulnerable in HD (Sotrel *et al.* 1993, Klapstein *et al.* 2001 & Spires *et al.* 2004) suggesting that there is both a proliferative and degenerative phase of alterations before the cell is finally submitting to death. The cause of these changes remains unknown but it is thought that they may reflect some primary abnormality in the regulation of dendritic architecture or a possible secondary compensation and decompensation effect for the alterations in the striatal circuitry. The early morphological changes in the medium spiny neurons have been described using both the Golgi and calbindin immunocytochemical methods (Graveland *et al.* 1985 & Ferrante *et al.* 1991). Changes observed in medium spiny neurons prior to any degeneration include dendritic remodelling which implies that these cells undergo a period of stress prior to death. Other changes seen in even

moderate cases of HD include the prominent re-curving of distal dendritic terminal branches, increased branching and increased number of dendritic spines. The degenerative atrophic alterations which were found in severe cases consist of truncated arbours, focal dendritic swelling and marked spine loss which is indicative of a prolonged period of degeneration in which the neuron is unable to support its processes and their physiological demands.

As well as pathology in the dendrites there has been some abnormalities seen in the axons and in the neurites which may be either axons or dendrites. Levels of synaptophysin, an axonal marker have been shown to be significantly reduced in HD brain insinuating the depletion of the medium spiny neuron local collaterals or the degeneration of striatal afferent terminals when they lose their target cells (Goto & Hirano 1990). The presence of dystrophic neurites have been widely seen and reported (Cammarata *et al.* 1993 and Jackson *et al.* 1995) these are abnormal processes which are not identifiable as either dendrite or axon. These processes are routinely seen in EM preparations of *cortex* in HD brain material and those of the mouse models investigated in this study, these are morphologically abnormal and stain for ubiquitin and ubiquitin hydrolase suggesting that degradation processes are taking place within them.

The morphometric data shows a quite dramatic reduction in the somal areas of neurons in the R6/2 mice, up to 50% in the marked cases. A lesser effect was observed in the R6/1 brains, and the difference was very subtle in the HD94 and HD80 mice. It was originally thought that the gross reduction in the size of the brain was due to cell death however in this study it was established that neurons were shrinking and the reduction could be directly attributed to this.

To investigate exactly where shrinkage was occurring Golgi impregnation studies were carried out. The finer structure of the neuron could be examined more thoroughly and as in several previous neuropathological studies of neurological conditions, more subtle changes in pathology were identified. The bulk of the brain's neuropil is comprised of dendrites the location, branching pattern and morphology are modified by experience and activity, which are

compromised in disease and trauma. Dendritic growth is crucial to the correct functioning of the brain as the dendritic form governs the number pattern and the type of synapses that a neuron establishes. It is the changes in these structures that give the earliest indication that there is serious dysfunction in the brain and so it is here that studies have concentrated for neuropathological clues. Cheng *et al.* (1997) looked at responses to lesions, Garey *et al.* (1998) studied changes in the schizophrenic brain and Irwin *et al.* (2000) found dendritic spine structure anomalies in the condition called Fragile X. Golgi studies have found that there are changes in the dendritic arbours of neurons in brains affected by Down's syndrome (Fiala *et al.* 2000) as the disease progresses, with Rett's disease (Leontovich *et al.* 1999 & Azmitia 2001) and forms of autism (Snow *et al.* 2008) showing similar pathology. Metabolic storage disorders such as Batten's disease (Chronister *et al.* 1995) have been shown to have major pathology highlighted by the use of this technique. Purpura *et al.* (1982) have linked the presence of varicosities with the disruption of microtubule organisation furthermore it has been thought by some groups working in this field that *htt* has a role in this system, and so such findings would have much wider implications on the role of the normal protein function. Perhaps an older technique such as the Golgi silver impregnation may yet shed new light on the pathology of HD giving new insight into the mechanisms of this disease.

### **6.1. Mangiarini/Bates Transgenic R6 Models**

In the end stage mice there is a marked difference in the *cortex* and *striatum* of the R6/2 mice, there are more clear patches where there are fewer impregnated neurons. This could be due to neurons becoming less able to hold the stain as the disease progresses. Also at first glance there seem to be missing layers of the *cortex*, namely layers III and V that are involved in cortico-striatal communication.

### 6.1.1. Striatal pathology

In most studies of HD the emphasis has been on that *striatum* where there is the most dramatic changes, these were discussed in the introduction pathology section in more detail (Chapter 1 section 1.6). Therefore the initial Golgi studies also concentrated in this region of the brain where extensive pathology is known to occur. Further studies were carried out on other populations of neurons, such as the *cortex*, *hippocampus* and *cerebellum*.

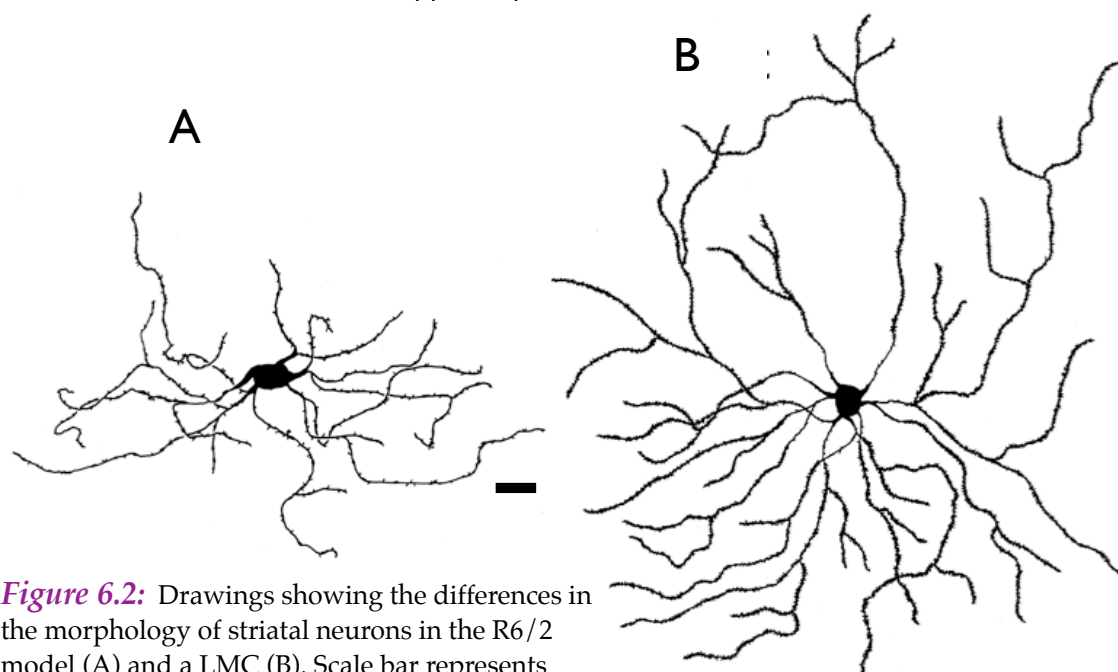
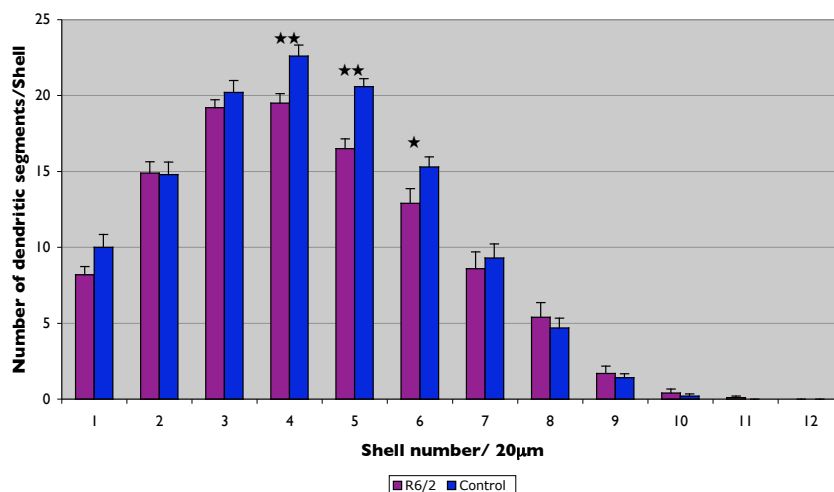


**Figure 6.2:** Drawings showing the differences in the morphology of striatal neurons in the R6/2 model (A) and a LMC (B). Scale bar represents 20 $\mu$ m.

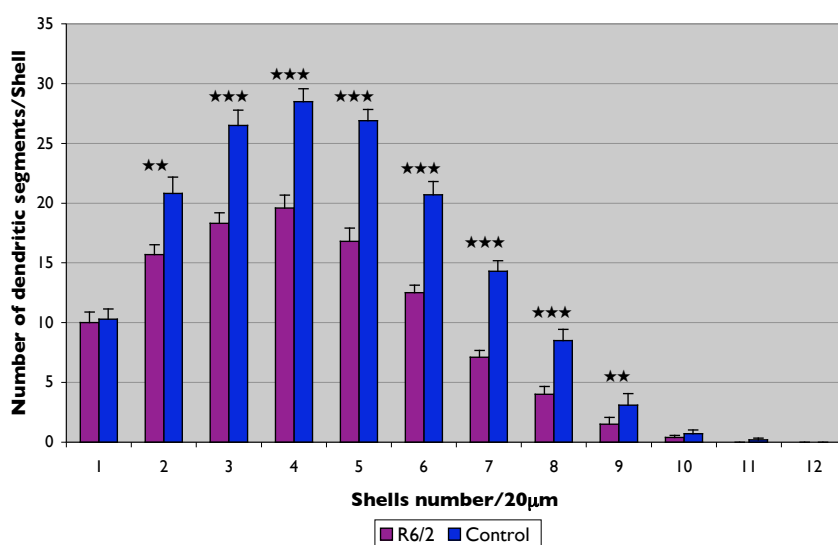
#### 6.1.1.1. Dendritic arbours

At the low power microscopy level there is an immediately observable reduction in the dendritic arbours, these appear to be quite markedly pruned back and the area over which they radiate dramatically reduced compared to the LMCs. A Sholl analysis (shown in [Figure 6.3](#) overleaf) was carried out to confirm this observation. It was found from these studies that the dendritic arbours grew fairly normally until the age of 8 weeks after which they appeared to be undergoing a pruning event, which continued until at end stage the R6/2 arbours were very much reduced. This would greatly reduce the extent to which the neuron is able to communicate and survive.

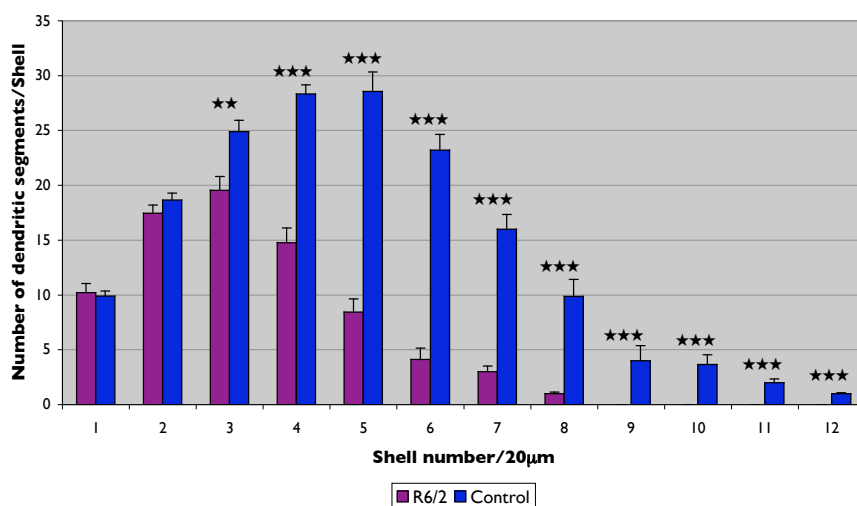
### Sholl analysis of medium spiny neurones in the R6/2 model of HD at 4 weeks of age



### Sholl analysis of medium spiny neurones in the R6/2 model of HD at 8 weeks of age



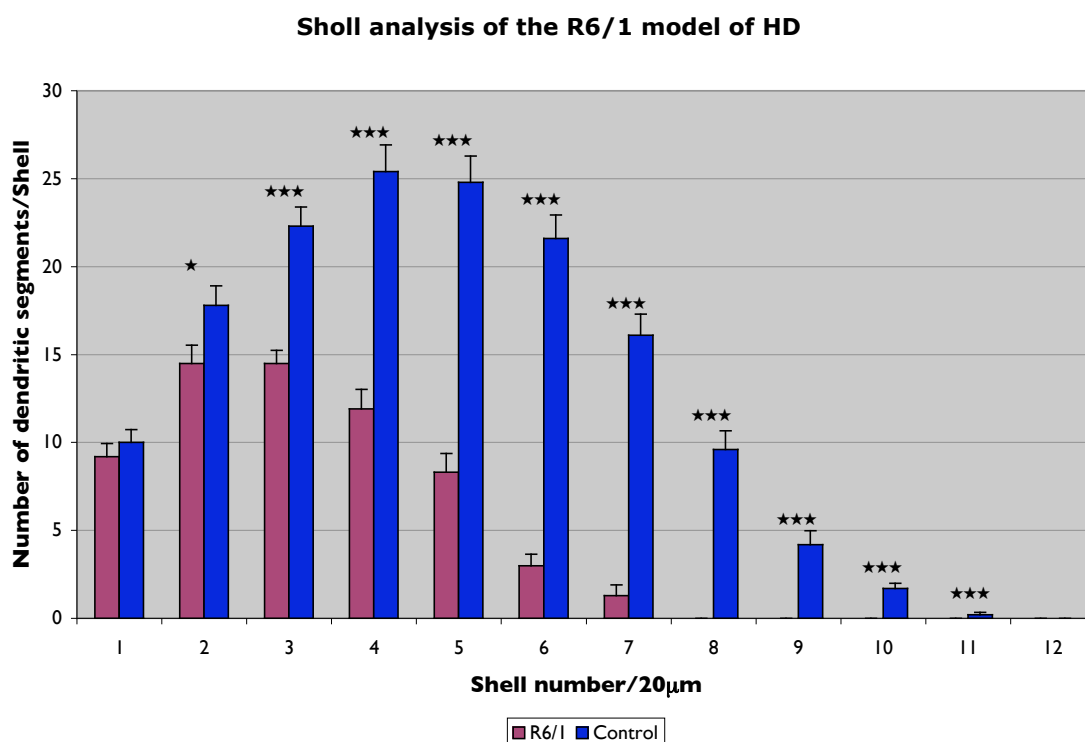
### Sholl Analysis of medium spiny neurones in the R6/2 model of HD at 12 weeks of age



**Figure 6.3:** Graphs showing Sholl analyses of the R6/2 model at 4, 8 and 12 weeks of age. For numbers of neurones measured please see section 2.6.3 on page 56 in Methods chapter. ★- $p < 0.05$ , ★★- $p < 0.01$  ★★★- $p < 0.001$  Student's t-test indicating a highly significant change between the somal areas of the R6/2 and littermate control.

The Sholl analyses of the R6/2 model in *Figure 6.3* on the previous page shows a detectable change in the dendritic arbour. At 4 weeks of age the appears to be an increased number of branches close to the cell body in the R6/2 compared with the LMC, however further out there appear to be more branches in the LMCs, suggesting that the arborisation of the R6/2 model is beginning to show signs of change and being compromised. At 8 and 12 weeks this effect is amplified and can be seen most explicitly at the 12 weeks timepoint, when the dendritic arbour has been severely reduced. The dendritic arbour has been pruned back in the R6/2 thereby reducing its connectivity capability to other neurons significantly.

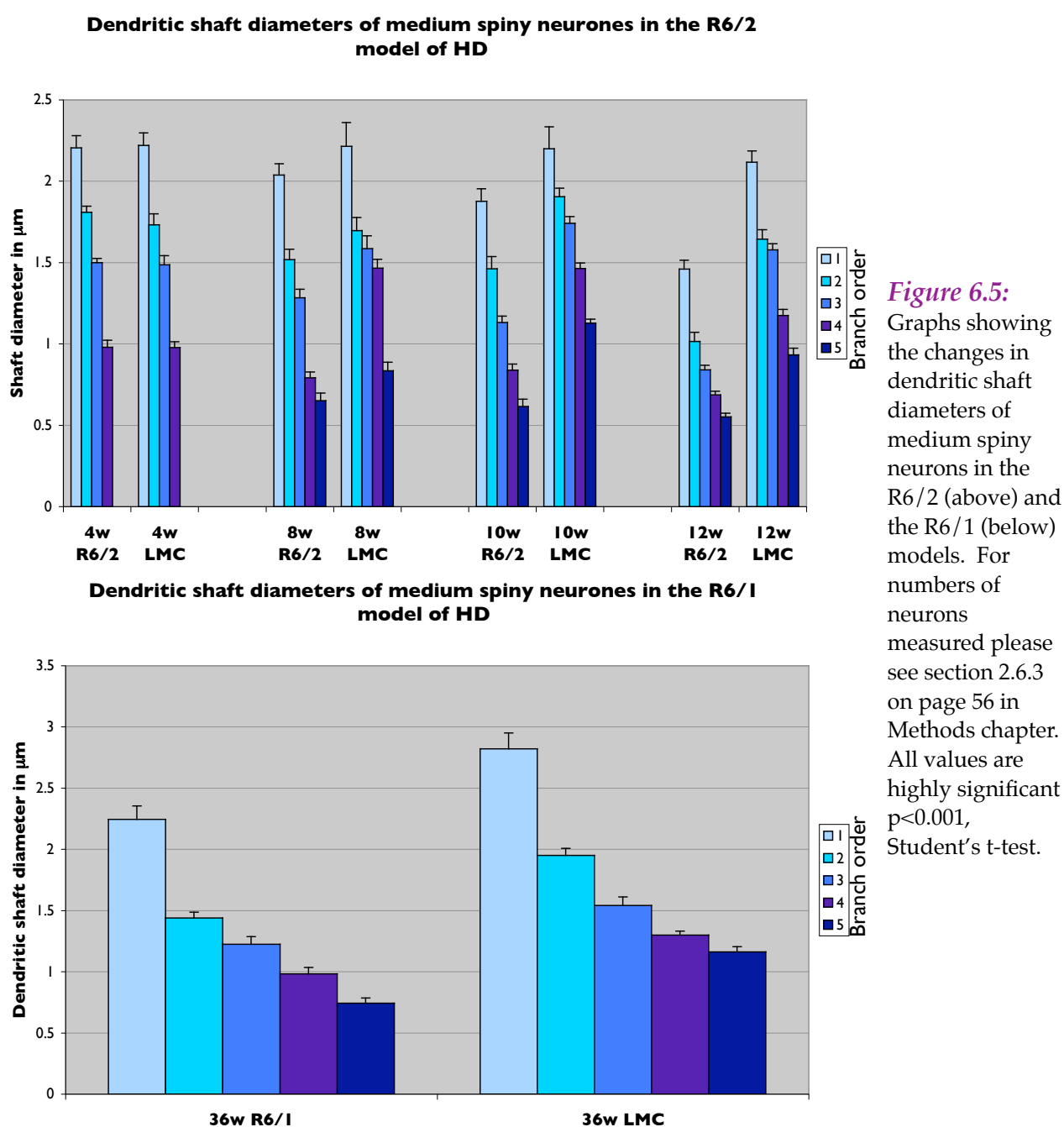
The R6/1 model has shown a similar change at end stage showing that similar pathological events are taking place in this model as are in the R6/2 as seen in *Figure 6.4* below. Additionally as these animals are much older perhaps the added variable of age needs to be considered, but as the LMC animals show clearly this is not the case.



*Figure 6.4:* Graph showing Sholl analysis of the R6/1 model at 36 weeks of age. For numbers of neurons measured please see section 2.6.3 on page 56 in Methods chapter. \* $p < 0.05$ , \*\*\* -  $p < 0.001$  Student's t-test indicating a highly significant change between the somal areas of the R6/1 and littermate control.

### 6.1.1.2. Diameters of dendritic shafts

At high power magnification of x100 the dendritic shafts appear much thinner and gracile than their LMCs, which are more robust and thicker. It was also much harder to find a length of dendrite stretching over 5 branch orders in the R6/2 neurons. Initial studies showed that there was at least a 50% decrease in the diameter of a 12 week R6/2 compared to the control animal. A more detailed study with increased number of animals and looking at differences over different branch orders, showed this phenomenon indeed to be correct as is shown in the graphs and drawings in *Figures 6.5 & 6.6* below.



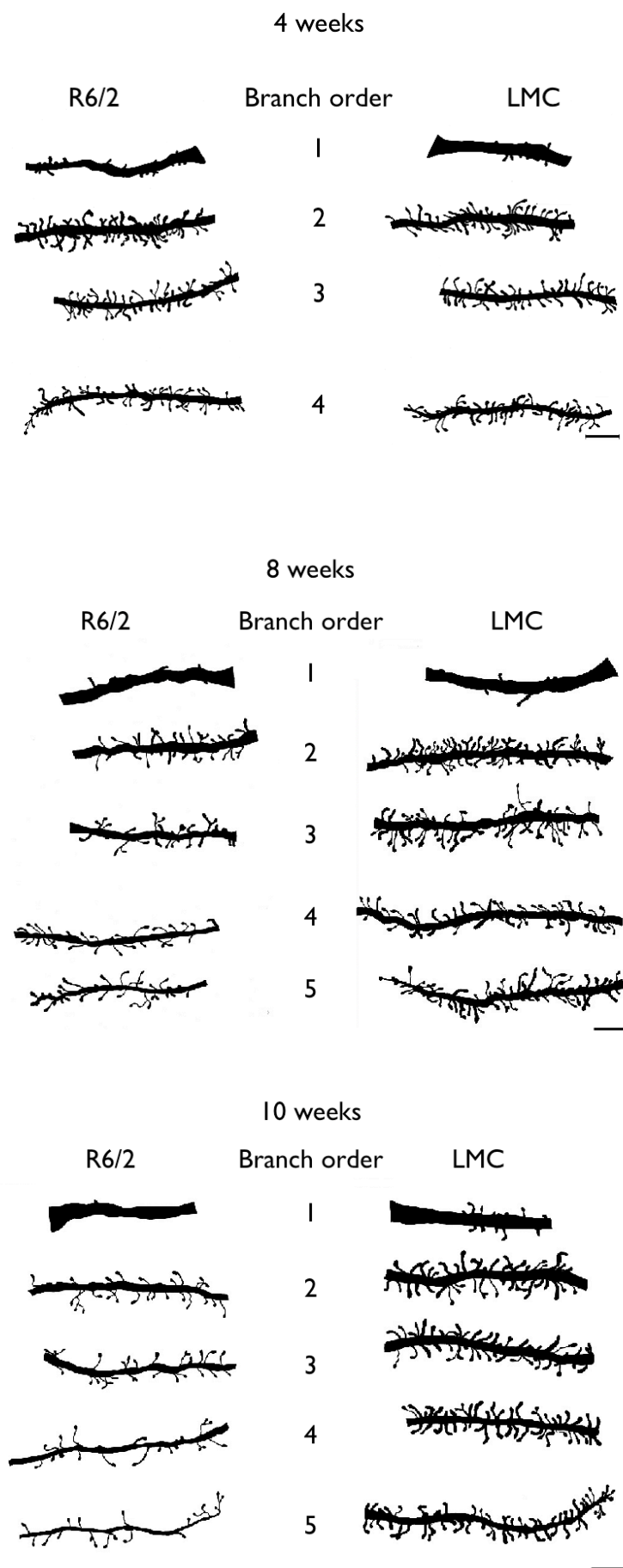


**Figure 6.6:** Camera lucida drawings of the dendritic branch segments of each order in the striatal neuron of the R6/2 model at 4, 8, 10 and 12 weeks of age. The scale bars represent 10 $\mu$ m.



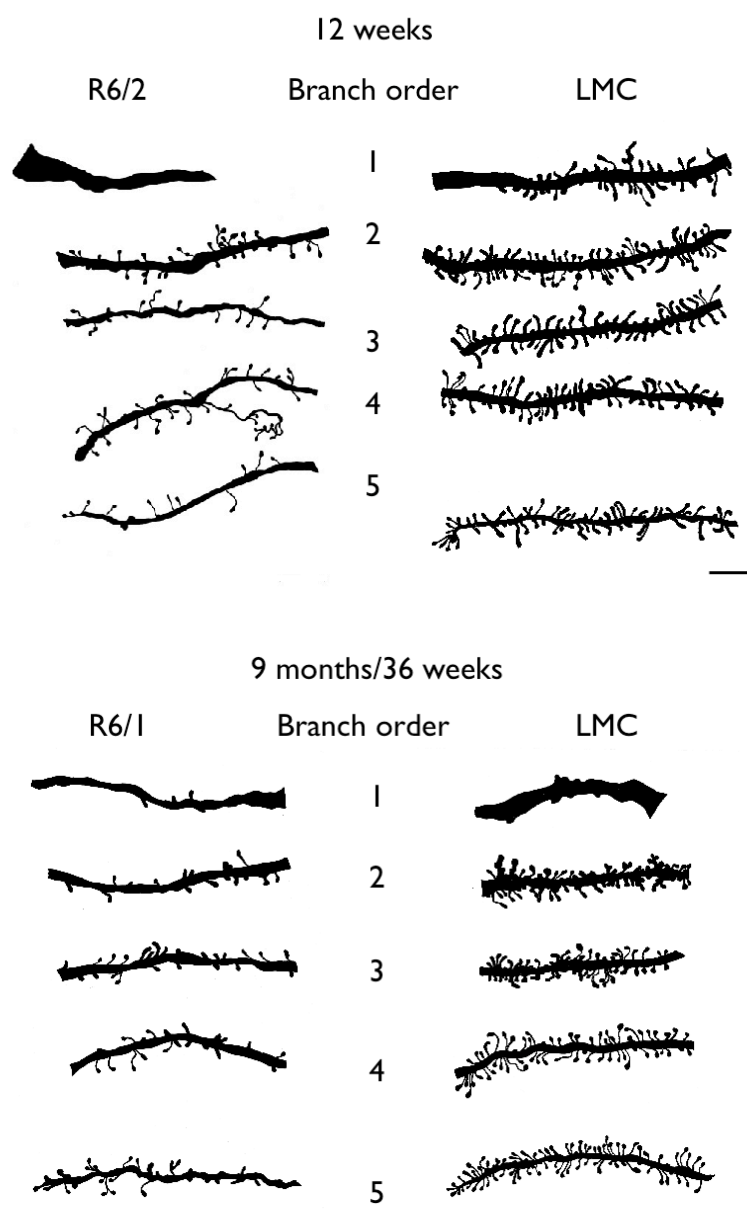


**Figure 6.7:** Camera lucida drawings of the dendritic branch segments of each order in the striatal neurons in the R6/1 model at 9 months or 36 weeks of age. This age is comparable with the HD94 model shown later on in this chapter in [Figure 6.19](#). The scale bars represent 10 $\mu$ m.

The drawings in [Figures 6.6 & 6.7](#) show sections of dendrite in the R6 models and do emphasise the difference in the gross appearance in their structures and level of spine density which is handled in more detail in the next section. Additionally the difference in the spine morphologies can also be seen some of which have been shown in [Figure 6.10](#) individual spines appear to be more thin and less stumpy which are associated with immature spines suggesting remedial sprouting. On the whole all the transgenic animals have a very ‘wispy-looking’ and ‘less fluffy’ appearance suggestive of a decrease in surface area on which synapses can form, therefore huge implications for the synaptic communication system of this region of the central nervous system.

### 6.1.1.3. Spine density

At first glance the most striking difference seen between the R6/2 and the LMC is the substantial loss of spines in the transgenes and the brush-like appearance of the LMCs. This dramatic denudation of dendrites appears to occur after 8 weeks when the overt expression of phenotype is detected culminating in sparsely spaced spines along the dendritic shaft at 12 weeks. This appears to be the case in all branch orders of dendrites but is more pronounced in the secondary branches, as they are hyper-spiny to begin with.

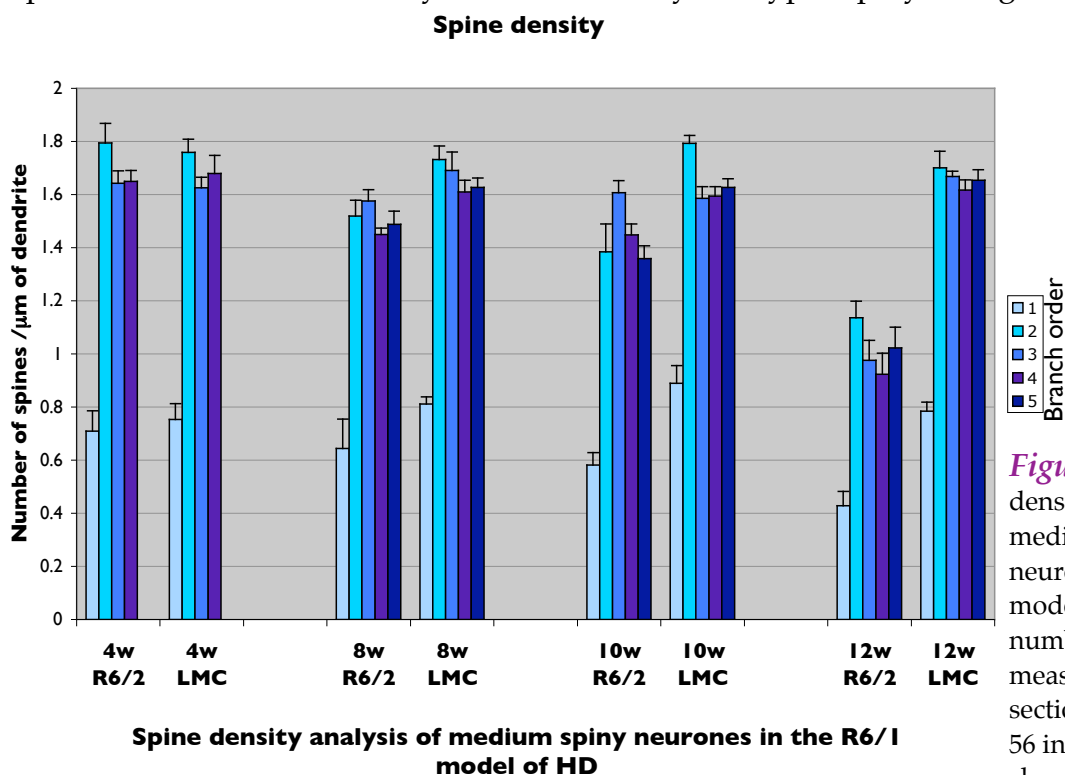
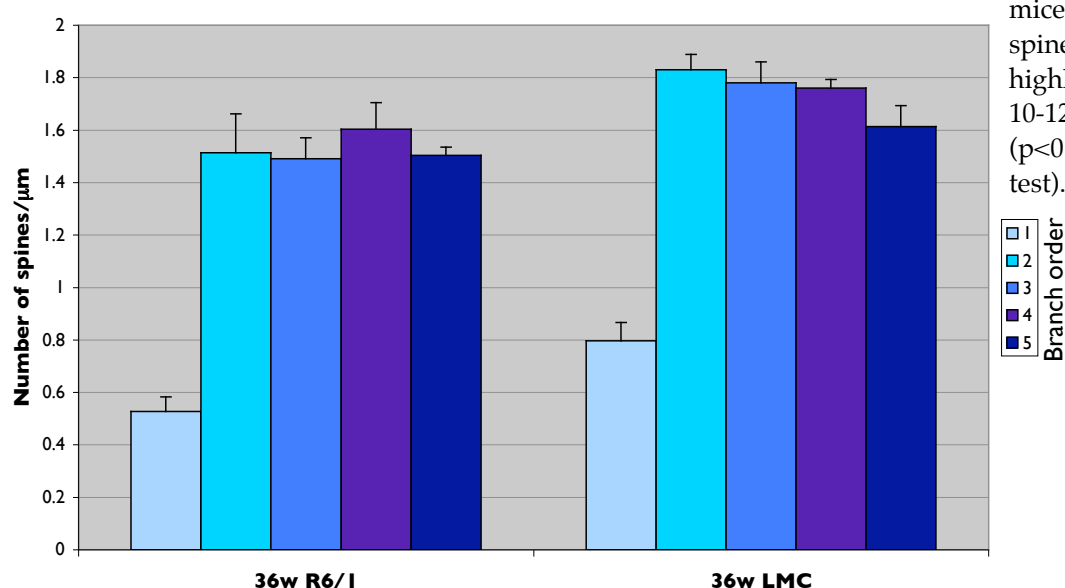


**Figure 6.8:** Spine density analysis of the medium spiny neurons of the R6 models of HD. For numbers of neurons measured please see section 2.6.3 on page 56 in Methods chapter. For the R6/2 mice the decrease in spine density becomes highly significant by 10-12 weeks of age ( $p < 0.001$ , Student's t-test).

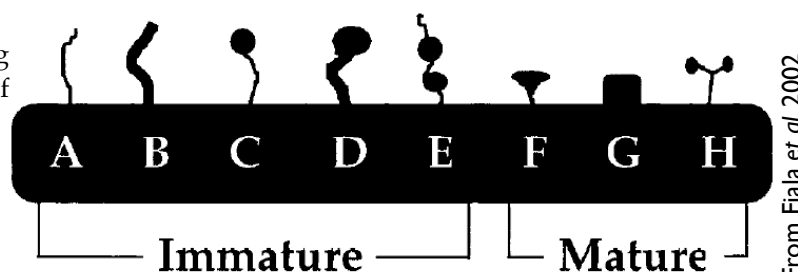


#### 6.1.1.4. Spine morphology & abnormal dendritic growths

The spines in the LMC animals at 12 weeks have very distinct shaft that grows off the dendritic shaft and a spine head at the end of this, both these are contacted by other neurons via synaptic boutons to set up communications. Spines in the R6/2 animals at 12 weeks are much finer and gracile in appearance and do not have such a defined head at the end of the spine. In some cases they appear to have degenerated into stumps on the dendritic shaft and in others they have branched out like a pair of antennae.

The range of spine morphologies that are observed have been identified in a scale to show the different forms of mature and immature spine shapes that are seen in the mouse when studying changes seen in fragile X syndrome (Irwin *et al.* 2002). The scale is shown below to give some idea of how much of a varied range there is in this type of pathology.

**Figure 6.9:** Diagram showing the different morphologies of spines in Golgi studies.

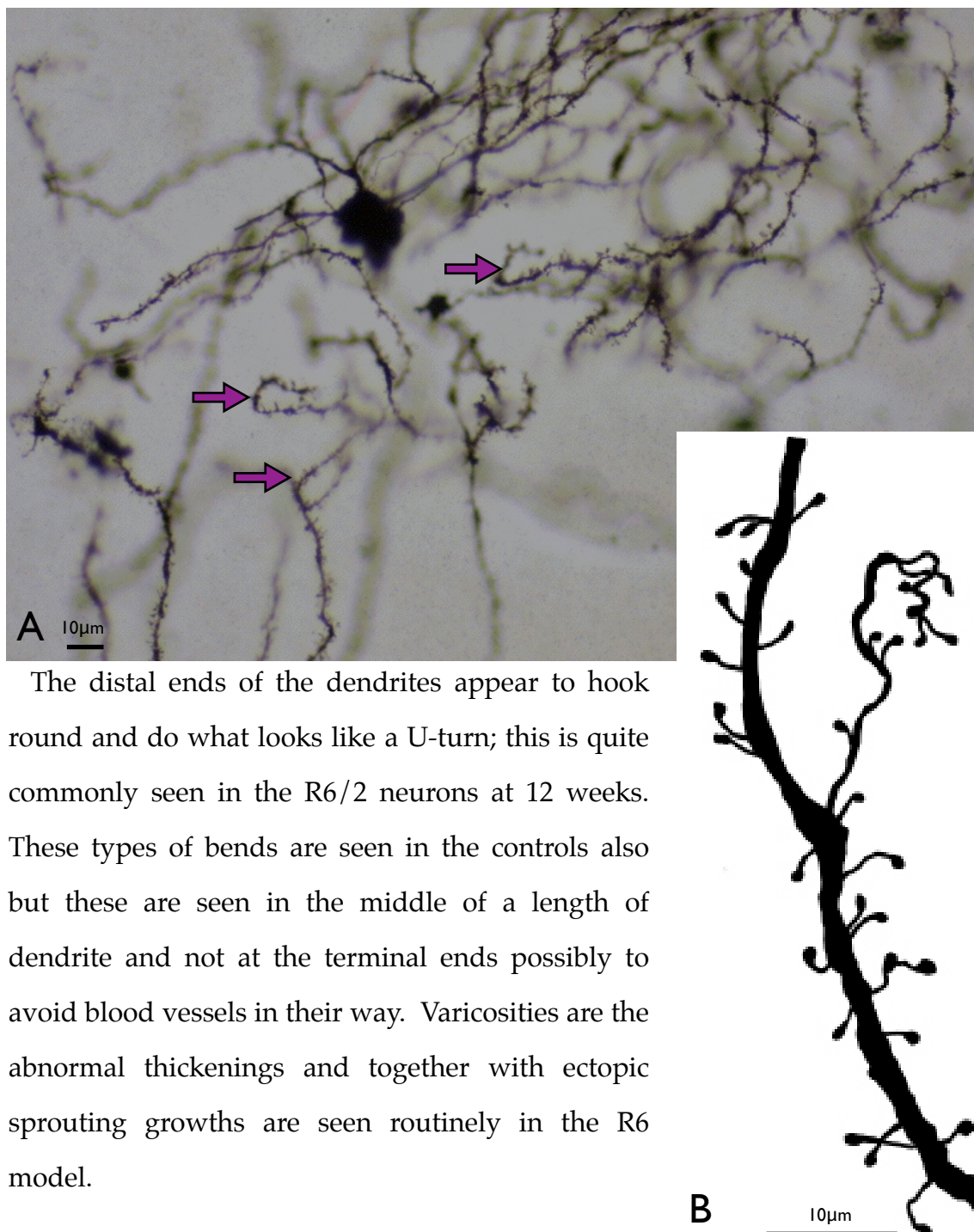


The range of different spines seen in the R6/2 mice is quite varied, on the one hand there are very gracile long spines and on the other there are stumpy more mature looking ones. Though it does appear that there are more stumpy mature spines present suggesting that maybe the dendrite is no longer capable of generating new spines which can form synapses. It has been established that dendritic spines are quite plastic structures remodelled quite frequently, it appears that by the end-stage of disease in the R6/2 mice at around 12 weeks this ability is severely compromised or lost completely.

It is very difficult to determine whether the abnormal growths are indeed dendritic or if they are very contorted spines that have got extra growths on them. Some spines look like they have whole branches growing off them.

Sprouting varicosities seen in human *postmortem* tissue shown at the beginning of this section of results (Graveland *et al.* 1985) are also seen in the 12 week R6/2. Some examples of these unusual spine morphologies and abnormal growths are shown in the figures below.

**Figure 6.10:** Photograph showing the different phenomena of sprouting and hooking as well as different morphologies of spines seen in Golgi studies of the R6 model in A the purple arrows show pronounced hooking. Drawing (B) shows the sprouting and varicosity effect also seen in the R6 mice as well as in human tissue see **Figure 6.1**. There are several different spine morphologies also seen on this drawn length of dendrite mostly immature forms seen in **Figure 6.9**.



The distal ends of the dendrites appear to hook round and do what looks like a U-turn; this is quite commonly seen in the R6/2 neurons at 12 weeks. These types of bends are seen in the controls also but these are seen in the middle of a length of dendrite and not at the terminal ends possibly to avoid blood vessels in their way. Varicosities are the abnormal thickenings and together with ectopic sprouting growths are seen routinely in the R6 model.

### 6.1.2. Giant Cholinergic neurons

This very small population of cells making up about 1% of the *striatum* appears to be spiny in murine brain whereas there is a lot of emphasis on them being aspiny in most neuroanatomy textbooks. The population of giant cholinergic cells are spared in the R6/2 model where they remain intact whilst neurons around them are affected. As this is a very small population and the Golgi process only allows 1% of the complete number of neurons present in the brain to be impregnated, the total number of these neurons seen in a brain is therefore quite low, however these observations have been made on these few cells and also commented on by other studies (Klapstein *et al.* 2001 & Morton *et al.* 2000).

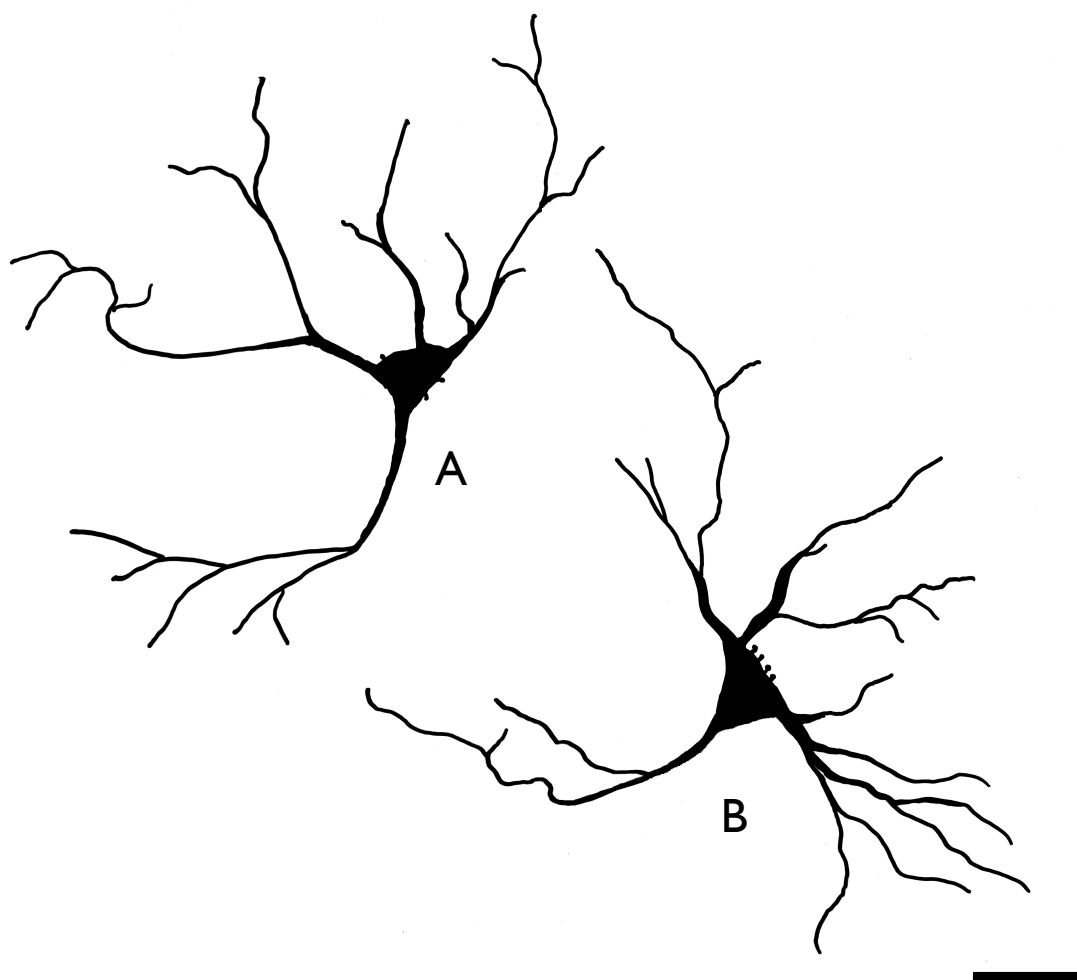


**Figure 6.11:** Drawings showing the giant cholinergic neurons of the R6/2 (B) and a LMC (A). The scale bar represents 25 $\mu$ m. There did not appear to be any differences between the two.

### 6.1.3. Cortical pathology

The most obvious pathology could be seen even at lower power magnification on the microscope, some layers of the *cortex* were depleted and these were found to be layers III and V. Neurons in these layers were found to exhibit the same pathology as the medium spiny neurons with decreased dendritic arborisation, dendritic diameters and dendritic spine density. It does appear that there is extensive pathology in the *cortex* in HD as highlighted by Sotrel *et al.* (1993) even though it is described as affecting the basal ganglia in the main. Changes of the levels of neurotrophins such as BDNF suggest that there are changes occurring in the *cortex* long before any changes have begun in the *striatum* (Zuccato *et al.* 2008). This idea suggests that the *cortex* is the primary source of pathology and therefore it is here that early changes should be investigated. These findings also suggest that there is some inherent property of pyramidal neurons that somehow render them more susceptible to early damage.

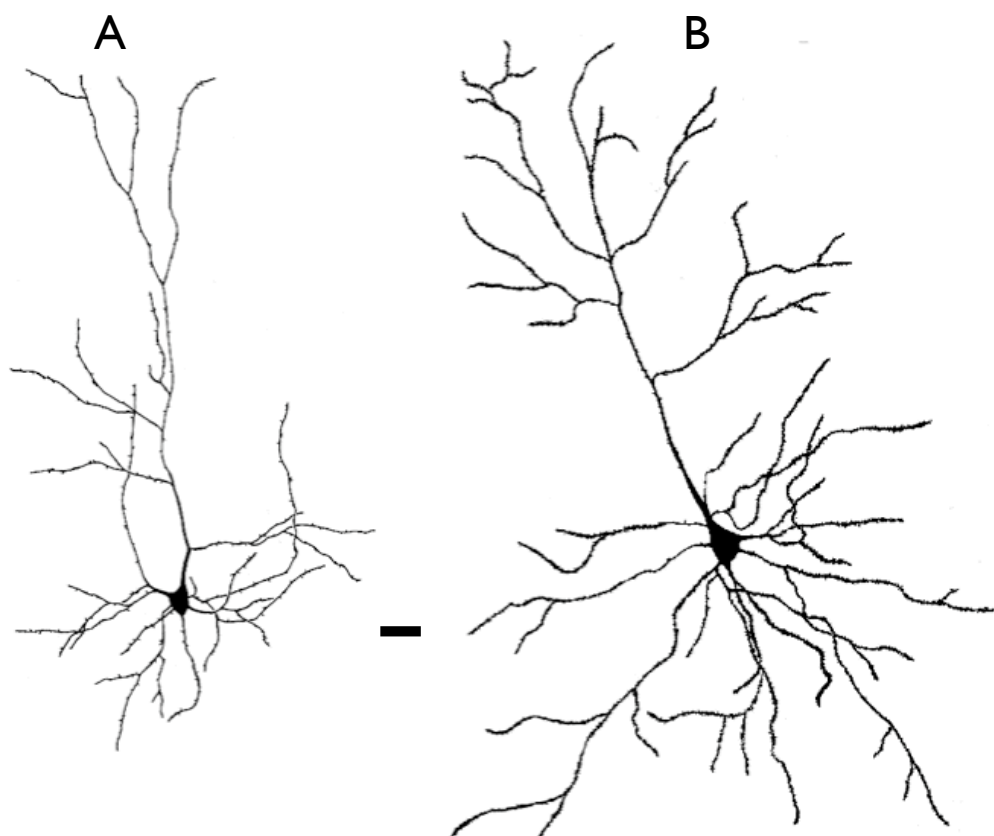


**Figure 6.12:** Drawings showing the differences in the morphology of cortical neurons in the R6/2 model (A) and a LMC (B). The scale bar represents 20 $\mu$ m. The mice were 12 weeks of age.

#### 6.1.4. Hippocampal cell pathology

This population of neurons is seen to have large inclusions by immunocytochemistry and is used in slice preparation experiments for electrophysiology studies (Klapstein *et al.* 2001). Some groups have shown cognitive impairments of hippocampal-dependent learning correlating to abnormal electrophysiological properties of CA1 neurons (Murphy *et al.* 1998) Hippocampal pyramidal neurons were also found to have the same changes as the cortical pyramidal neurons namely decreased dendritic arborisation, dendritic diameters and dendritic spine density.

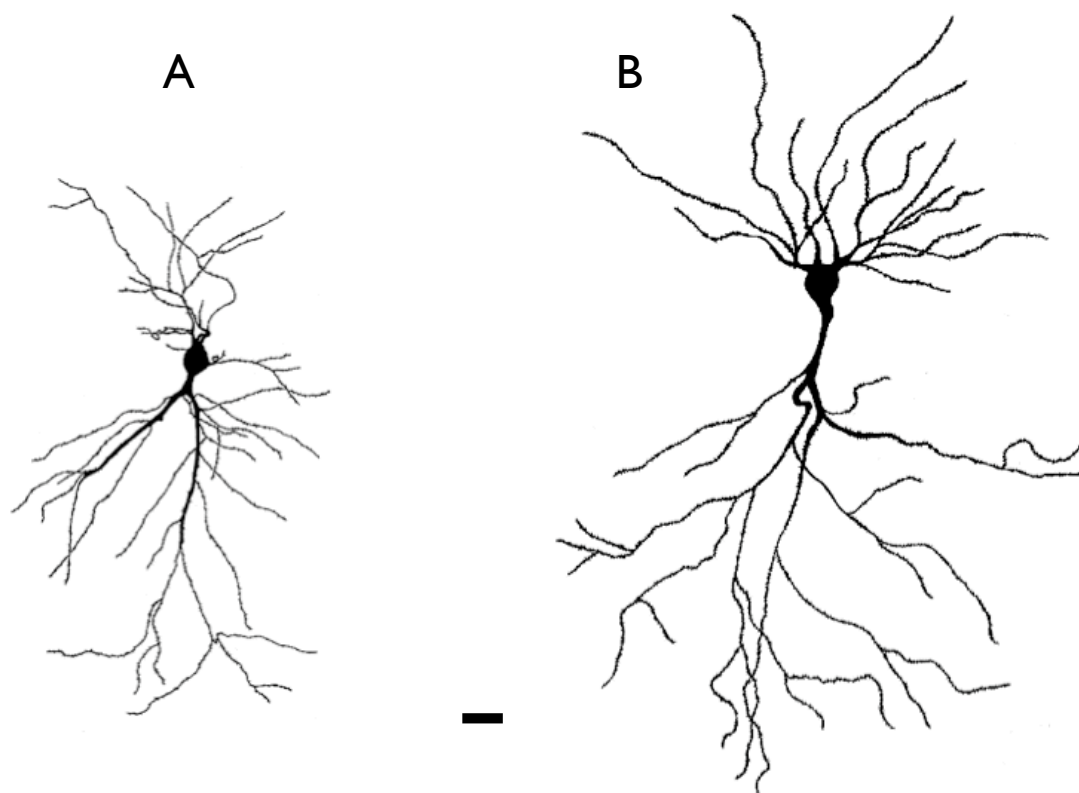


**Figure 6.13:** Drawings showing the differences in the morphology of hippocampal pyramidal neurons in the R6/2 model and a LMC. The scale bar represents 20 $\mu$ m. The mice were 12 weeks of age.

### 6.1.5. Purkinje cell pathology

Purkinje cells were found to be affected in HD, with a reduced density in a study by Jeste *et al.* in 1984. In this study a similar reduction in density was found in the R6/2 mice and the morphometric study showed that these cells had shrunk by about 40%, not as pronounced as in the cortical or the striatal neurons but quite significant none the less. Purkinje cells also seem to die in a different manner to the striatal and cortical neurons (Turmaine *et al.* 2000). It would not be unreasonable to expect some pathology in Golgi impregnated tissue. However it appears that these cells are quite difficult to impregnate and perhaps take a lot longer as they are so much larger than other cell populations. Some pictures of the cells found in the R6/2 and HD94 mice (these serve as controls as they are under a forebrain specific promoter and the *cerebellum* is unaffected) are shown below.

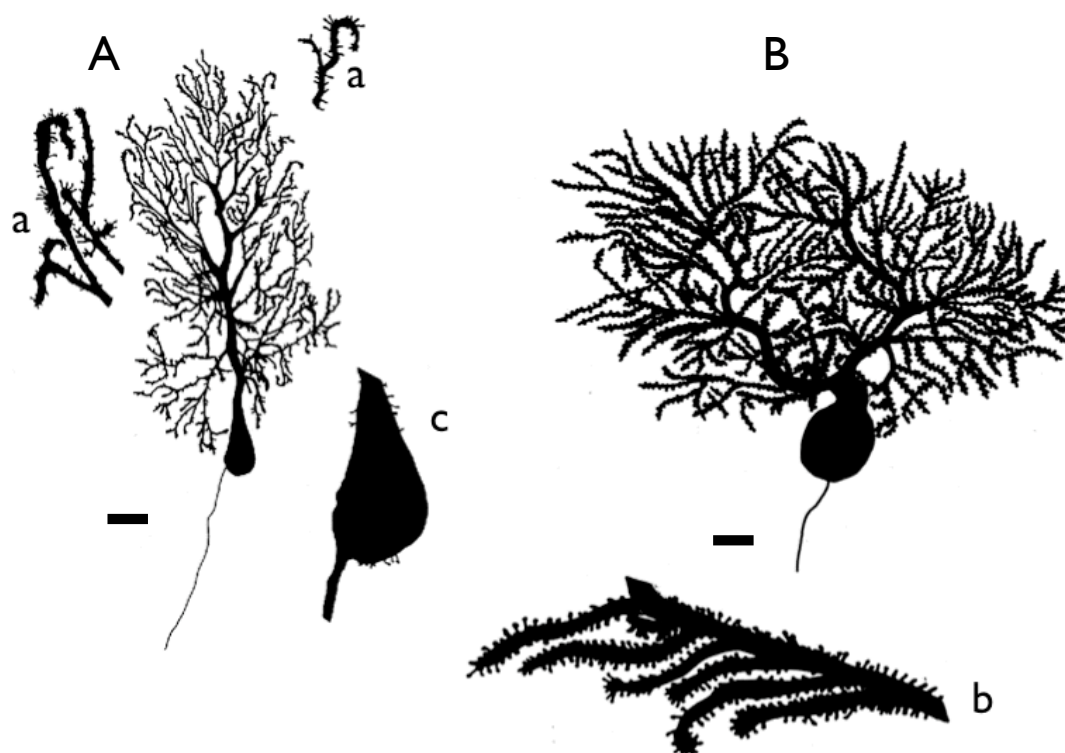


**Figure 6.14:** Drawings showing the differences in the morphology of Purkinje cells of the cerebellum in the R6/2 model at 12 weeks of age (A) and an HD94 model at 36 weeks of age (B). Higher power drawings show 'hooking' or curving at the distal ends (a) and the normal distal ends (b) additionally of interest are the spines on the cell body (c). The scale bar lower power drawings represents 20 $\mu$ m.



### 6.1.6. Glia

These are seen in the Golgi impregnated sections as woolly masses around the neurons. There seem to be more of them around unhealthy looking cells in the *striatum* and in the layers of the *cortex* with shrinking cells, suggesting that some form of gliosis is taking place. However the immunocytochemical studies imply that this process does not appear to be taking place, at least not to the extent that has been suggested in human studies (see Chapter 8).

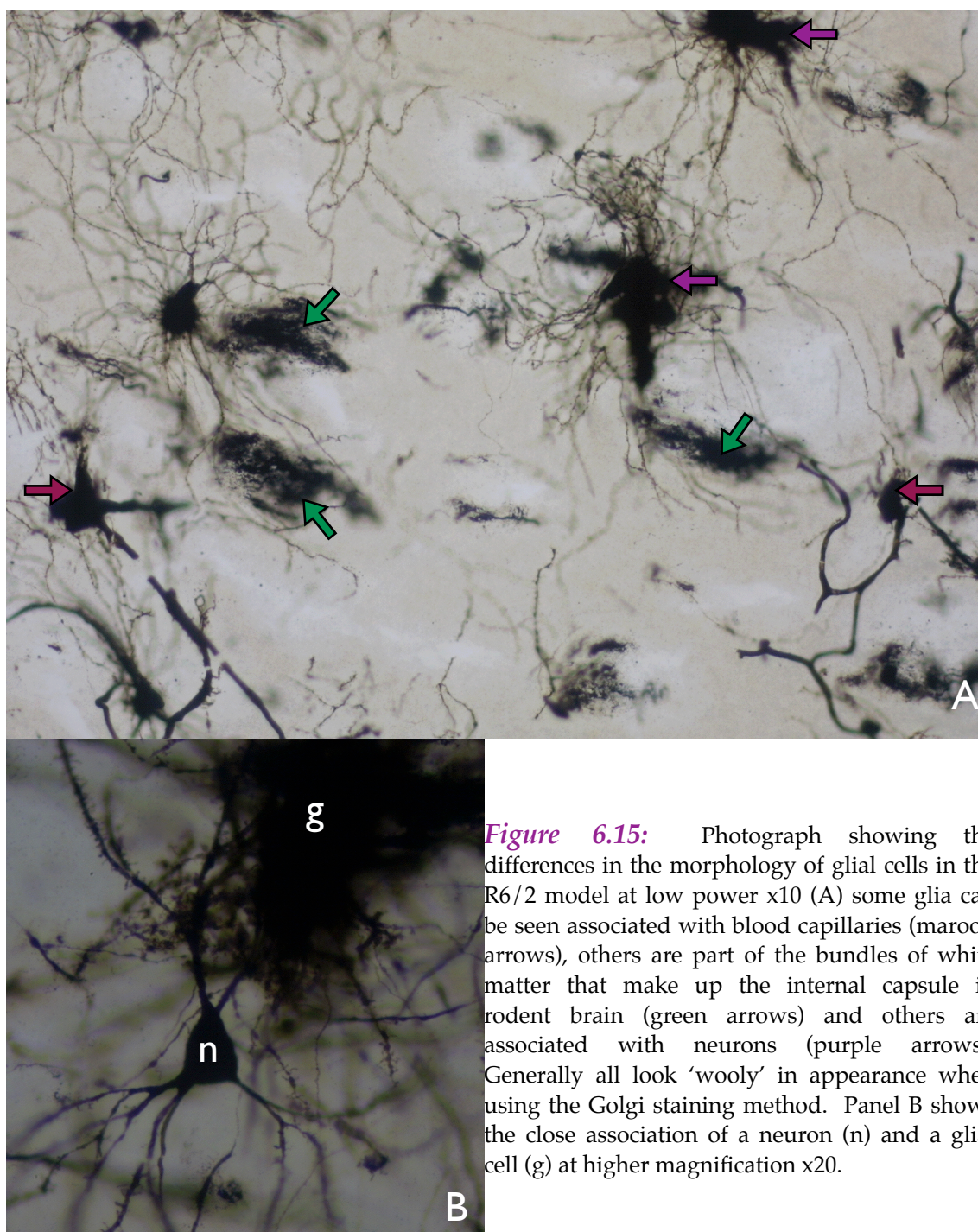


**Figure 6.15:** Photograph showing the differences in the morphology of glial cells in the R6/2 model at low power x10 (A) some glia can be seen associated with blood capillaries (maroon arrows), others are part of the bundles of white matter that make up the internal capsule in rodent brain (green arrows) and others are associated with neurons (purple arrows). Generally all look 'woolly' in appearance when using the Golgi staining method. Panel B shows the close association of a neuron (n) and a glial cell (g) at higher magnification x20.

### 6.1.7. Olfactory bulbs

Samples of these bulbs were used in this study more out of curiosity than anything else. Personal communication with people maintaining mouse colonies had revealed that perhaps transgenic mice showed signs of olfactory impairment. Impregnation of this tissue was not as good as with other areas samples but neurons did seem to be more truncated in the transgenes than in the LMC animals as shown in the figure below. It appears that these affected cells are the mitral neurons, which are a population of large pyramidal-looking neurons. Other populations of cells appear not to be affected to any great extent including the large numbers of astrocytes present in the olfactory bulb.

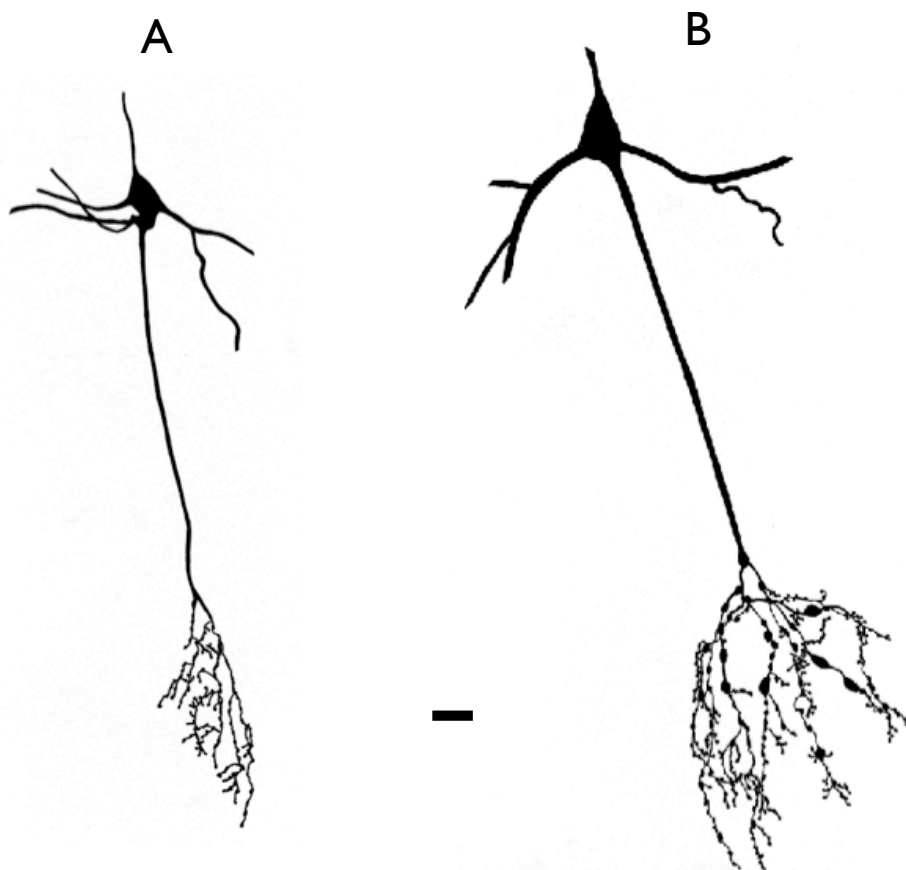


**Figure 6.16:** Drawings showing the differences in the morphology of mitral cells of the olfactory bulb in the R6/2 model (A) and a LMC (B). The scale bar represents 20 $\mu$ m.

## 6.2. Yamamoto HD94 Conditional Model

The majority of the pathology seen in this model has been in the *cortex*, but little difference was seen in the cellular structure of this region in this analysis.

### 6.2.1. Striatal pathology

These mice showed no major changes between the LMCs and the transgenic animals to warrant a full study like the one carried out in the R6 lines where there were obvious changes. The LMCs and the transgenes were very similar to the controls in the other models suggesting that there were indeed no discernible changes as seen in the figure below.

#### 6.2.1.1. Dendritic arbours

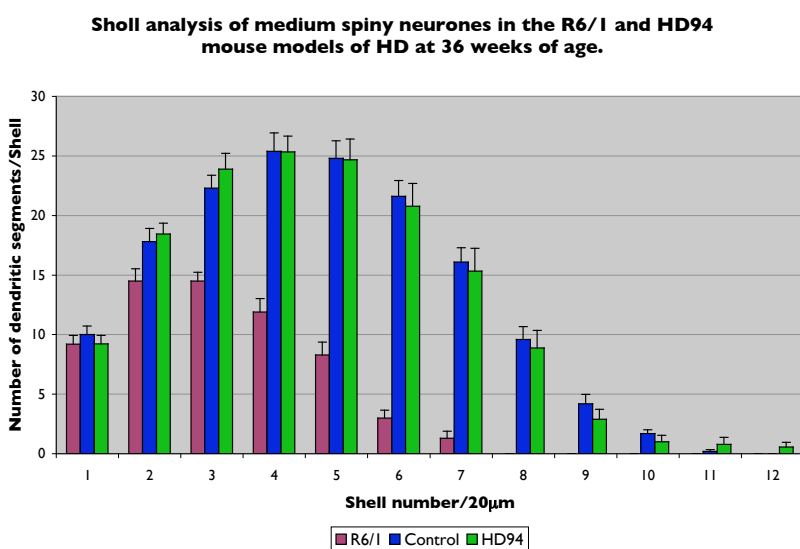
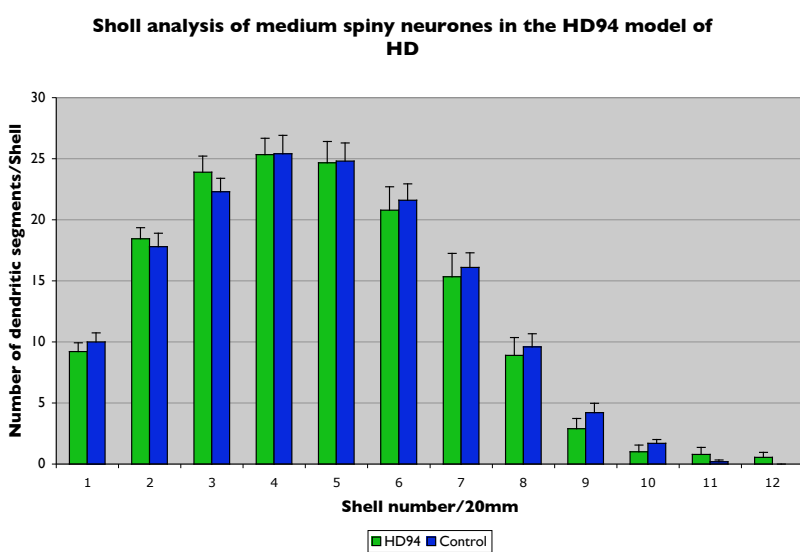


**Figure 6.17:** Sholl analyses of the HD94 model and comparison with the R6/1 model at the same age to emphasise the pathology. For numbers of neurons measured please see section 2.6.3 on page 56 in Methods chapter. There were no significant differences between the HD94 model and the littermate control using Student's t-test. This is highlighted by the R6/1 model shown in the lower figure in which the animals are of the same age and have highly significant changes.

### 6.2.1.2. Diameters of dendritic shafts

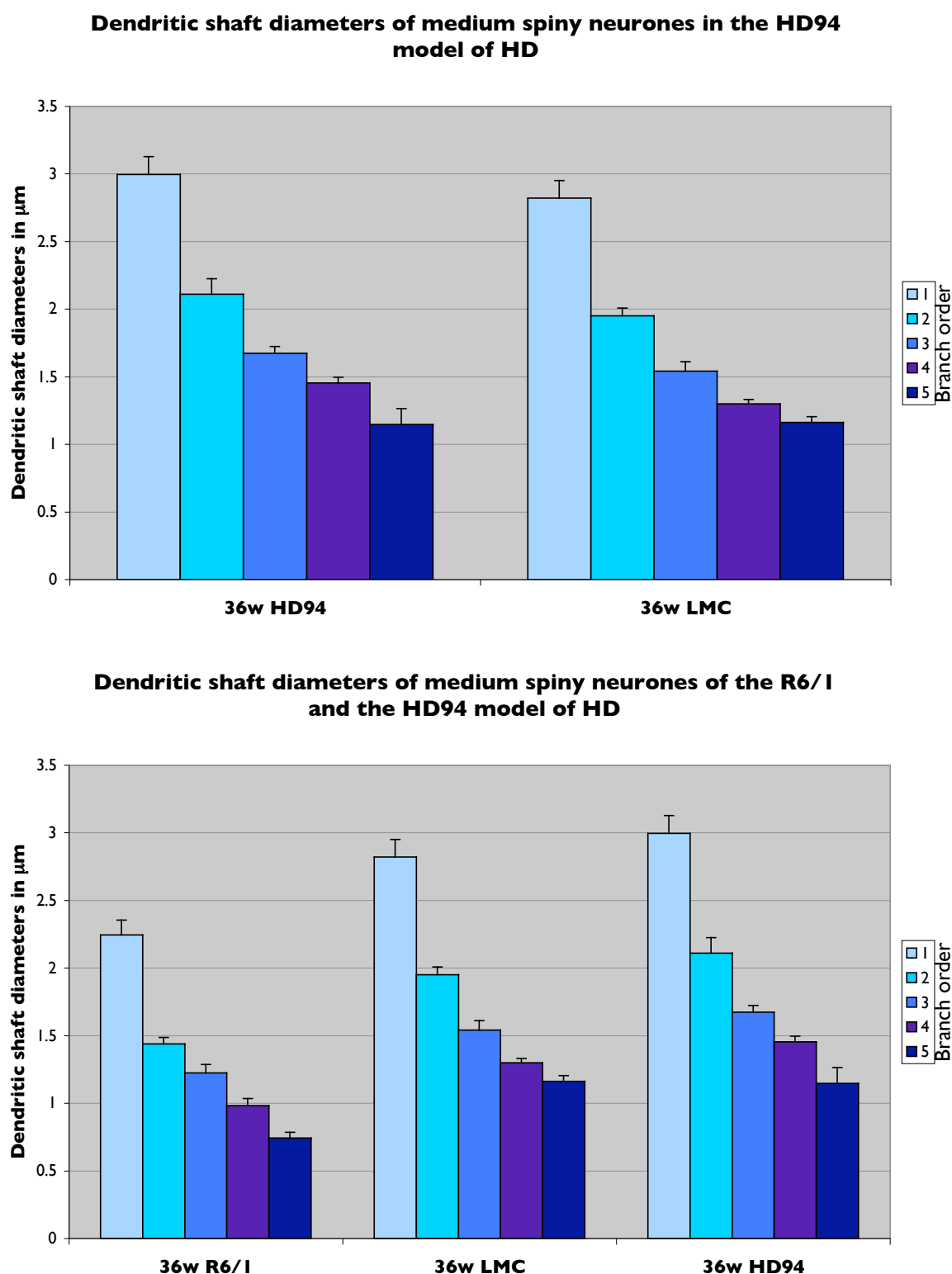


**Figure 6.18:** Graphs showing the dendritic shaft diameters in the HD94 model and comparison with the R6/1 which is the same age. For numbers of neurones measured please see section 2.6.3 on page 56 in Methods chapter. There were no significant differences between the HD94 model and the littermate control using Student's t-test. This is highlighted by the R6/1 model shown in the lower figure in which the animals are of the same age and have highly significant changes.

The dendritic shaft diameter parameter in the HD94 model shown in the graphs above, appears to be behaving similarly to the effect seen in the Sholl analysis whereby it appears to be slightly greater than the control animals and not at all reduced as in the R6/1 animals of the same age. This effect can also be seen in the drawings of the dendritic segments below in *Figure 6.19*. However there may be some subtle changes in the dendritic spines in that they do appear to be more gracile than the control spines some of which do look more stumpy and more mature. The different types of spines have been discussed earlier and shown in *Figure 6.9*. There does not however appear to be as pronounced a denudation effect as seen in the R6 models as the dendritic segments do appear to possess a substantial cover of spines and therefore it can be assumed that neuronal communications are not as compromised in this model.

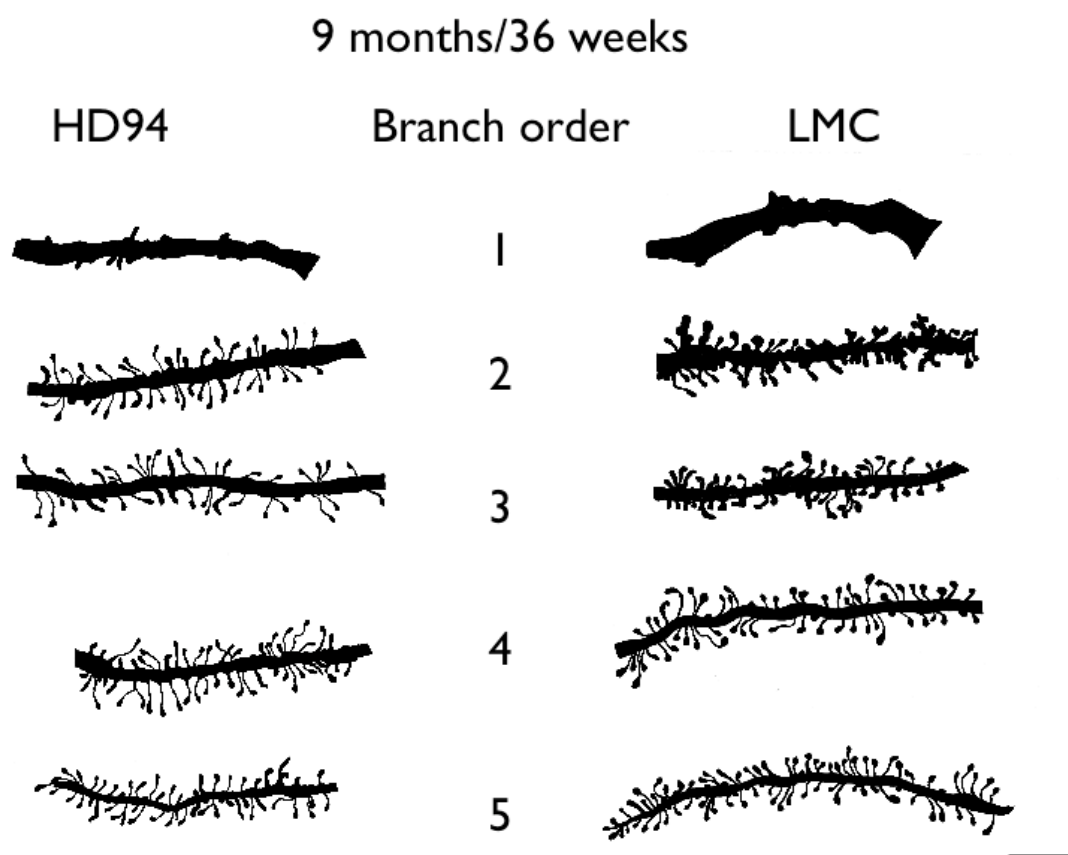


**Figure 6.19:** Camera lucida drawings of the dendritic branch segments of each order in the striatal neurons of the HD94 model at 9 months or 36 weeks of age showing dendritic morphology of segments of Golgi impregnated medium spiny neurons. The scale bars represent 10 $\mu$ m.

### 6.2.1.3. Spine density

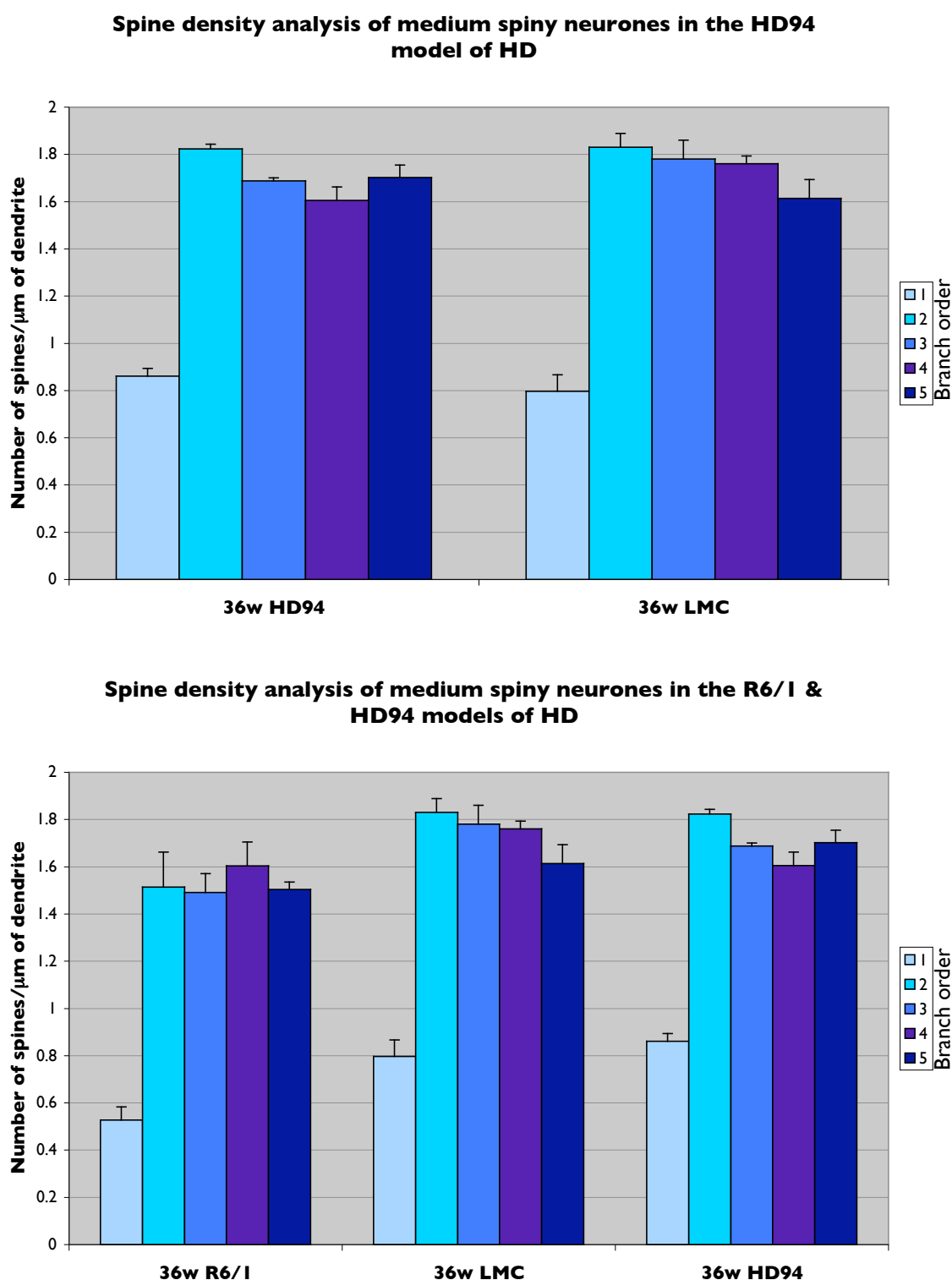


**Figure 6.20:** Graphs showing spine densities of dendritic branches in the HD94 model (above) and comparison with the R6/1 (below) which is the same age. For numbers of neurons measured please see section 2.6.3 on page 56 in Methods chapter. There were no significant differences between the HD94 model and the littermate control using Student's t-test. This is highlighted by the R6/1 model shown in the lower figure in which the animals are of the same age and have highly significant changes.

The spine density graphs in *Figure 6.20* on the previous page show that once again this model has defied the hypothesis and behaved in an anomalous way. Whereas it was expected that the dendritic arbours, shaft diameters and spine densities all decrease with disease progression, in this model these parameters have either remained the same or behaved in the opposite manner. The Sholl analysis showed that the dendritic arbour of this model appears to expand instead of contract shown in *Figure 6.17*, dendritic shaft diameters are very similar to the LMC animals shown in *Figure 6.18* and the drawings of dendritic segments in *Figure 6.19* show perhaps the only pathology in the gracile nature of the spines. These differences are in stark contrast to changes observed in the R6/1 model of the same age where all these parameters show dramatic pathology which is why wherever possible they have been presented additionally in the figures as a comparison.

Therefore in the Golgi studies this model has not yielded any results that will shed light on the collective information on the pathology of the induced HD condition in the mouse. More disappointing perhaps was the lack of effect seen with the administration of the DOX analog which was to reverse the pathology, as there was no baseline pathology of the HD94 in this study it seemed irrelevant to include results from the HD94 +DOX animals which would serve only to cloud the already muddied waters of this particular murine model of HD.

### 6.3. *Shelbourne Knock-in Model*

Golgi studies on this mouse model were carried out in three different types of mouse, the full-length knock in, truncated knock-in and the control showing changes in the background lines. Additionally there are lines on different background strains, which have appeared to make a difference in many other models. As most of the pathology is seen in the *striatum* it would be expected that the majority of the changes would be seen in this region with little or no effect in other regions. As the truncated knock-in model appears to have a more potent pathological effect it would also be expected that most of the changes seen with the Golgi technique would be seen in these mice with a lesser amount of change seen in the full-length knock-in.

The Golgi impregnated sections of this model were disappointing, it appeared they had not impregnated as well as the sections from the other two models had done. Perhaps this was due to the animals being several months older than those in the other two models investigated in this study. In the original studies using the Golgi method carried out by Cajal uses very young animals, often before myelination had completed, suggesting that age does make a difference to the quality of impregnation that is achieved.

#### 6.3.1. *Striatal pathology*

Impregnation was especially poor in the *striatum*, possibly due to the central location of this region of the brain and these brains being processed as a whole and not cut into smaller blocks. However despite these problems some data was obtained from these brains, it was possible to find the rare fully impregnated medium spiny neurons in the *striatum* and perform some measurements on these to be comparable to the other two models also studied.

The medium spiny neurons in the HD80 model appear to be very similar in appearance to their age matched LMCs, with very little in the way of pathology such as that seen in the R6/2 mice or the subtle changes seen in the HD94 mice. The disease pathology in these mice is very limited, which is not entirely an



unexpected result as these animals are just exhibiting the first behavioural symptoms of HD. The other brain regions such as the *cortex*, *hippocampus*, *cerebellum*, all appear to be normal with no discernible changes from the controls from this and other models.

### 6.3.1.1. Dendritic arbours

#### Sholl analysis of medium spiny neurones in the HD80 mouse model of HD

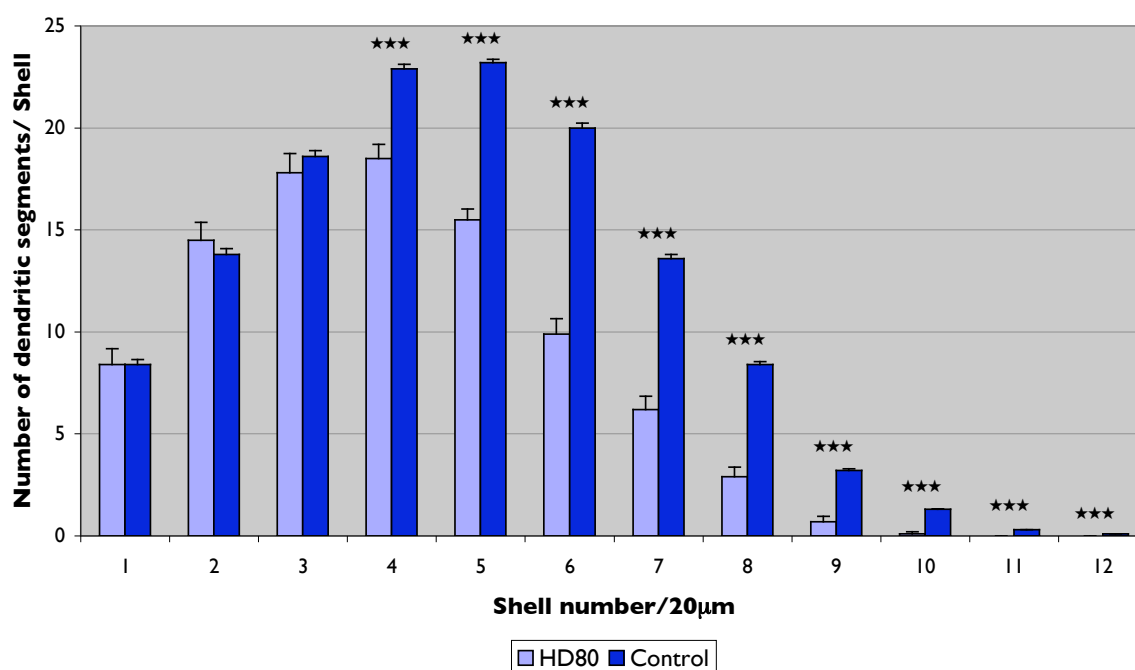


**Figure 6.21:** Graph showing the Sholl analysis for the HD80 model at 116 weeks of age. For numbers of neurons measured please see section 2.6.3 on page 56 in Methods chapter. \*\*\*-  $p < 0.001$  Student's t-test indicating a highly significant change between the HD80 and littermate control.

The Sholl analysis shown in the figure above shows a definite pruning effect in this model similar to that seen in the R6 models, suggestive of similar loss of connectivity in neural communications however the range of symptoms observed in the models is very different. It would be easy to attribute these findings to old age only the LMC animals of the same age show no pathology. Perhaps connectivity is not compromised in the same way as the other parameters studied show subtle changes and not marked ones as in the R6 models. The HD progression is working at a much slower rate in these animals however the important point is that it is showing pathology albeit a mild one.

### 6.3.1.2. Diameters of dendritic shafts

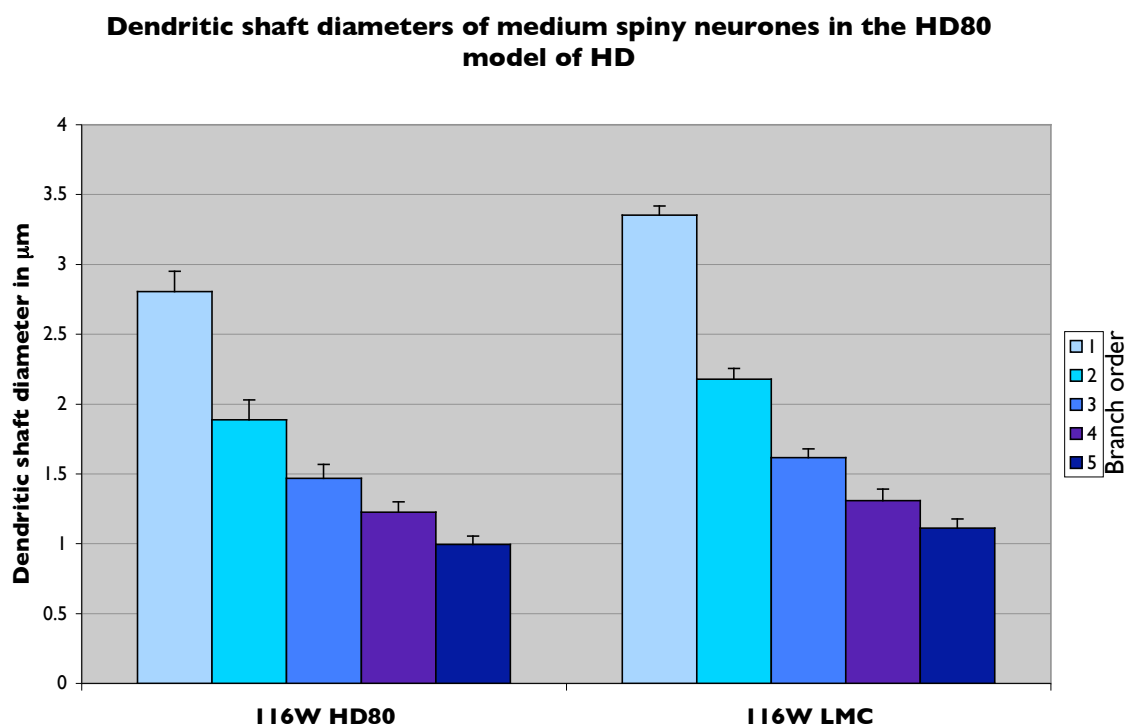


**Figure 6.22:** Graph showing the dendritic shaft diameters for the medium spiny neurons in the HD80 model at 116 weeks of age. For numbers of neurons measured please see section 2.6.3 on page 56 in Methods chapter. ★★★ -denotes  $p < 0.001$  Student's t-test indicating a highly significant change between the shaft diameter of the HD80 and littermate control.

The dendritic shaft diameters show that there is a noticeable change in the diameters of primary and secondary dendrites but a much milder change in the more distal orders of dendrite. This would suggest that the thinning of the dendrites happens from the cell body outward and not from the distal dendrites inwards. But when pruning is taken into consideration it appears to happen from the distal dendrites inwards. These changes imply that there are different condensation processes occurring in this disease pathology. Generally the diameters are larger across the board when compared with the other models this may be due to age, the neurons have had longer to establish mature dendritic arbours and connections which may be therefore more resistant to degeneration. These are all speculative ideas, but what is apparent is that the changes seen in this model are more subtle and similar to the earlier changes seen in the R6/2 mice and more importantly there is a definite pathology present which is remarkable given the mild phenotype.

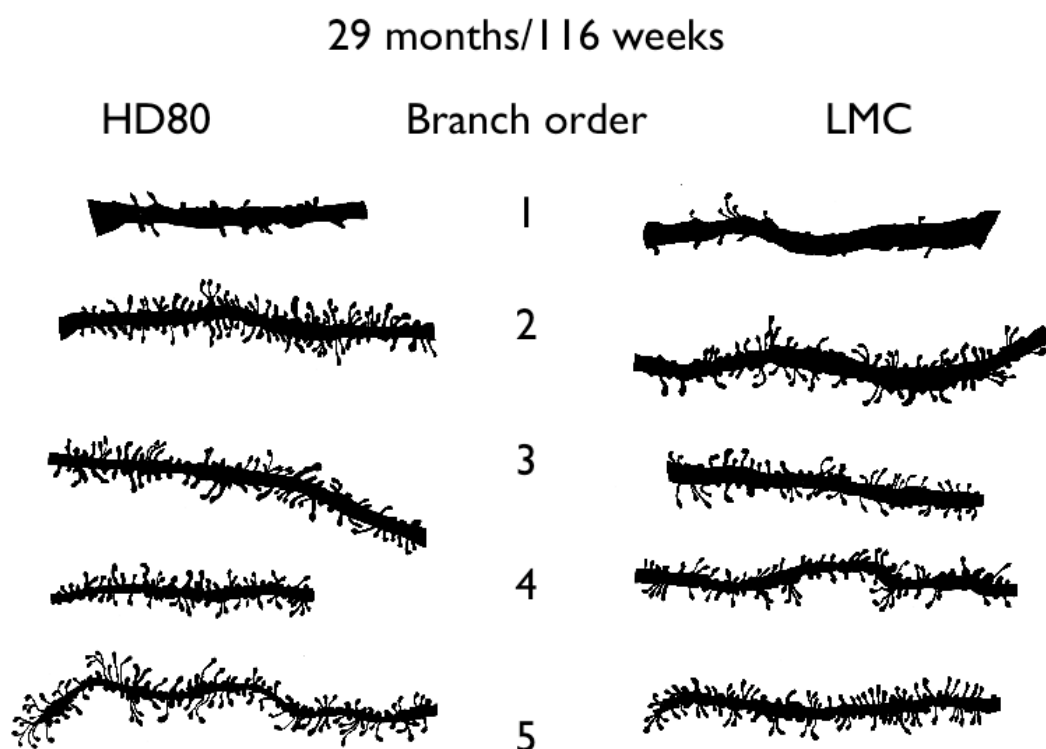


**Figure 6.23:** Camera lucida drawings of the dendritic branch segments of each order in the striatal neurons of HD80 model at 29 months or 116 weeks of age showing dendritic morphology of segments of Golgi impregnated medium spiny neurons. The scale bar represent 10 $\mu$ m.

The drawings of the dendritic branches show that there is very little difference at first glance all the sections appear to have similar shaft diameters and spine density with the same range of spine morphologies. The individual spines all appear to have a defined head and shaft component and are not too many of the varied forms of mature spines that are seen in the R6 models which suggests that the ability to produce new spines and maintain plasticity in the system has not been compromised. The graphs of the various analyses carried out in this study do show that there are some subtle changes in the knock in animals. The graph showing changes in spine density overleaf in [Figure 6.24](#) emphasises the subtle nature of change in this model where there really is little variation but importantly that there is some present. Being the most genetically accurate model the findings of this model are perhaps the most interesting to see how they compare to findings in *postmortem* human material.

### 6.3.1.3. Spine density

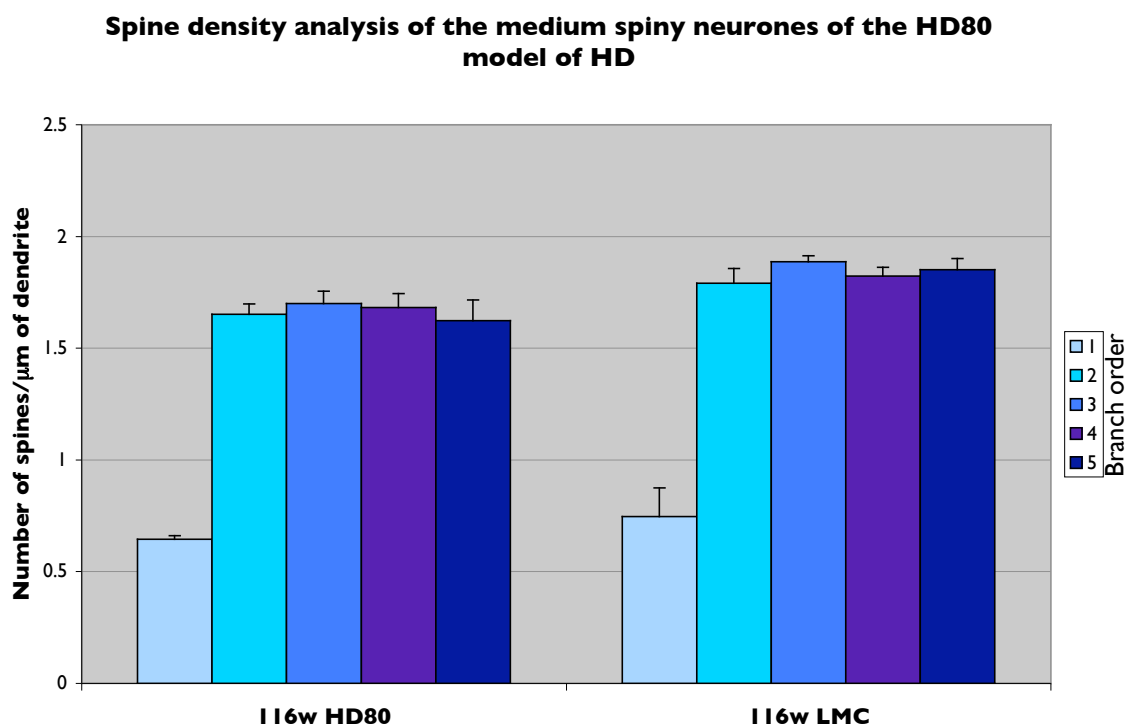


**Figure 6.24:** Graph showing spine density analysis for the HD80 model at 116 weeks of age. For numbers of neurons measured please see section 2.6.3 on page 56 in Methods chapter. There were no significant differences between the HD80 model and the littermate control using Student's t-test indicating a highly significant change between the shaft diameter of the HD80 and littermate control.

There seems to be a slight reduction in spine density across the whole range of dendritic branches which was not so apparent in the drawings in [Figure 6.23](#) on the previous page. Clearly this model is not in the hyperspiny phase of the pathology described in the human studies ([Graveland \*et al.\* 1985](#)) which is thought to precede the denudation of the dendrites which these findings may be the beginnings of. It would seem quite appropriate for this beginning of the denudation phase to coincide with the first behavioural symptoms that are seen in both human and the induced mouse versions of this condition.

Studying this model with the Golgi silver impregnation method turned out to be disappointing and trying to impregnate material from older animals may prove harder to achieve but would perhaps show more pathology. However being at the edge of the natural lifespan of the mouse there may be other pathology at work which may skew findings.

#### 6.4. Summary of results

Of all the mouse models studied using the Golgi silver impregnation method the R6/2 mice showed the most changes in pathology, however not all of these changes were the same as those seen in the human material studies. This finding seemed to be therefore asking more questions than getting answers and conclusions. There are dramatic changes seen in the medium spiny neuron population of the R6/2 model such as the reduction in dendritic arbourisation and shaft diameters, severe denudation in some sections, immature spine morphology and abnormal growths and contortions at the terminal ends of dendrites. Other striatal populations such as the giant cholinergic neurons remain unaffected and relatively healthy in end stage animals. In the human studies the medium spiny neurons appear to be hyperspiny and have more varicosities and contorted growths with not such a pronounced reduction in the dendritic arbour. This would suggest that there might be similar changes going on in these two types HD manifestations that are most definitely not identical. As the R6 lines are not a genetically exact model of HD these results are understandable and somewhat remarkable in the likeness to the disease making them valid to learn more about the disease mechanism by extrapolation. The results of the Shelbourne model show that there are indeed several changes seen in both the human studies and in this study that show that the genetic accuracy can give rise to the same pathology.

The gross brain pathology of the HD94 brains appears to be normal and all neuronal populations also appear to be unaffected. The medium spiny neurons have intact dendritic arbours, normal dendritic shaft diameters and spine densities. There is some “hooking” on the terminal ends of dendrites but no varicosities or sprouting growths. The failure of this model to give a pathological difference using this technique suggests that any changes may be negligible as there have been subtle differences picked up in other models. This result also suggests that the subtle disease phenotype reported in these mice

may be due to age or other model design factors, which cannot be guessed at this point.

Another murine model of HD has also been investigated using the Golgi impregnation method and was found to have some different changes to those seen in the three models studied here. The HD89 model is completely different to those in this study in that it has been engineered quite differently, with different promoters, background and repeat length all of which can contribute in their own independent way to the resultant phenotype, this is discussed further in the discussion chapters. Studies of this particular model using a similar method (Guidetti *et al.* 2001), report that they too have denudation of dendrites and reduced shaft diameters like that seen in the R6/2 model, but additionally they find proximal thickening of the cortical neurons. This phenomenon is also found in all the models investigated in this study but it is also seen in the controls, suggesting that this is not an exclusive phenotype to the diseased state.

At the end of this study we are left trying to explain these results and with a number of questions for further studies. How is it that the pathology seen is so varied and is it all due to differences in genetic engineering? Why are the changes seen in these models so different from those seen in human studies? Are there any presymptomatic cues, which may be used as an indication of whether the disease process is taking place? The pruning phenomenon does indeed appear to be happening markedly in the R6 models and more subtly in the HD80 model. These changes can be seen more obviously in the [Figure 6.25, 6.26 & 6.27](#) in the following two pages. When taken in comparison to the study in human material by Graveland *et al.* (1985), these findings are remarkably similar showing the pruning and the 'hooking' effect in some instances. This overall pattern of degeneration does appear to be part of the disease pathology, however the HD94 model once again does not conform to this pathology but appears to be unaffected by the pruning effect, but perhaps does exhibit some hooking in the distal dendrites (seen in some of the medium spiny neurons).



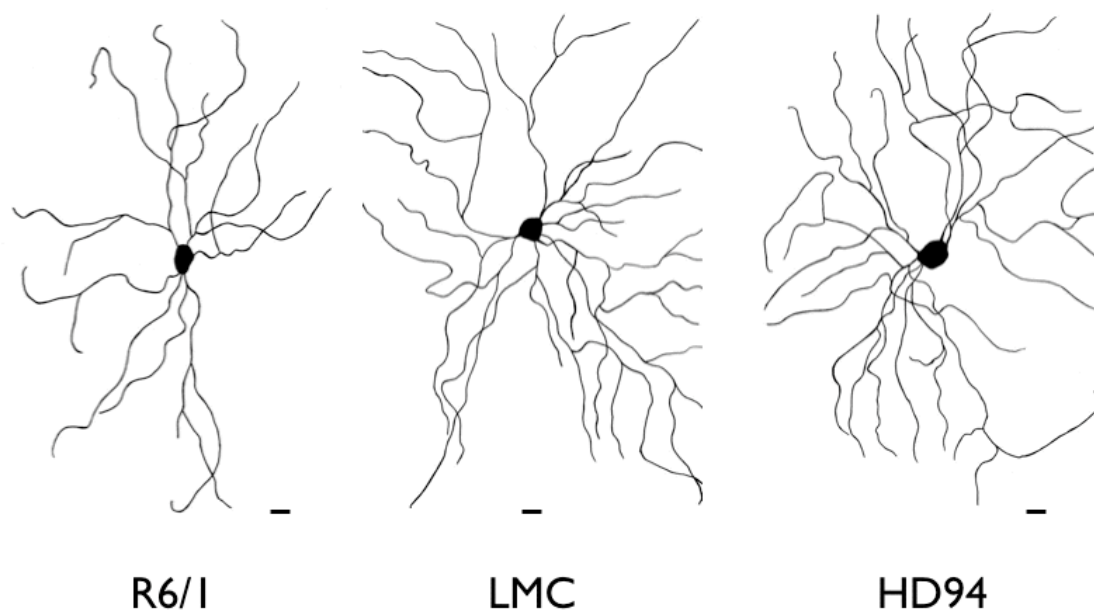


**Figure 6.26:** Drawings showing the dendritic arbours of medium spiny neurons for the models studied at 36 weeks/9 months of age. Notice how the R6/1 arbour is much more reduced and pruned in comparison with the HD94 which appears very similar to the control. The scale bar represents 10  $\mu\text{m}$

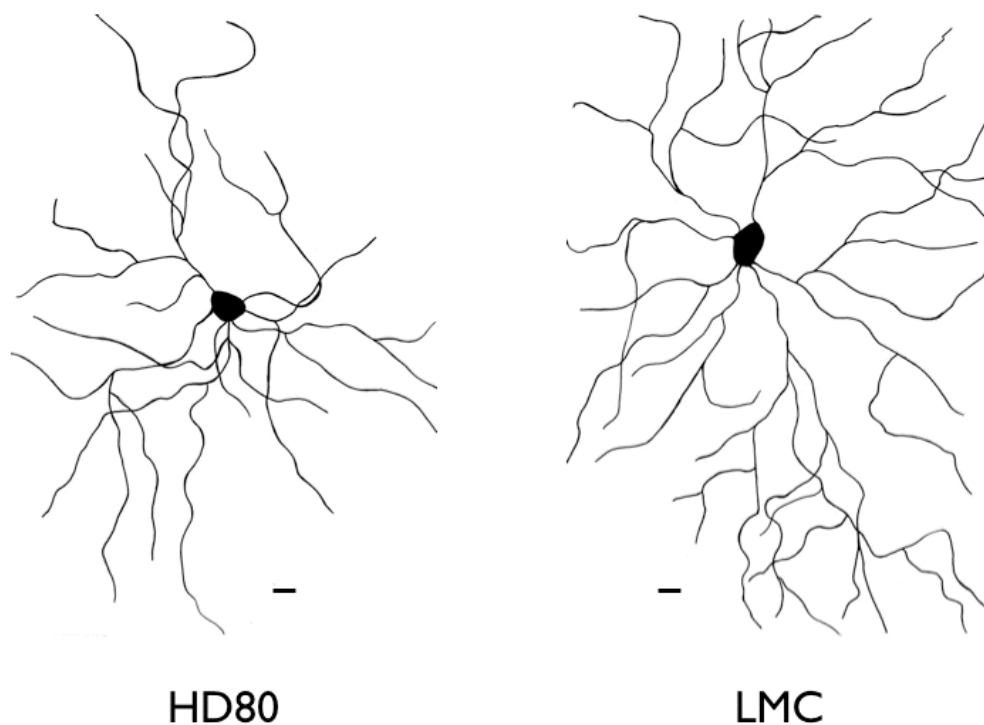


**Figure 6.27:** Drawing showing the dendritic arbours of medium spiny neurons in the HD80 model with the integrated fragment and LMC at 116 weeks/29 months of age. The drawing is of the most severe case that could be found and therefore has some pruning that is noticeable. The scale bar represents 10  $\mu\text{m}$



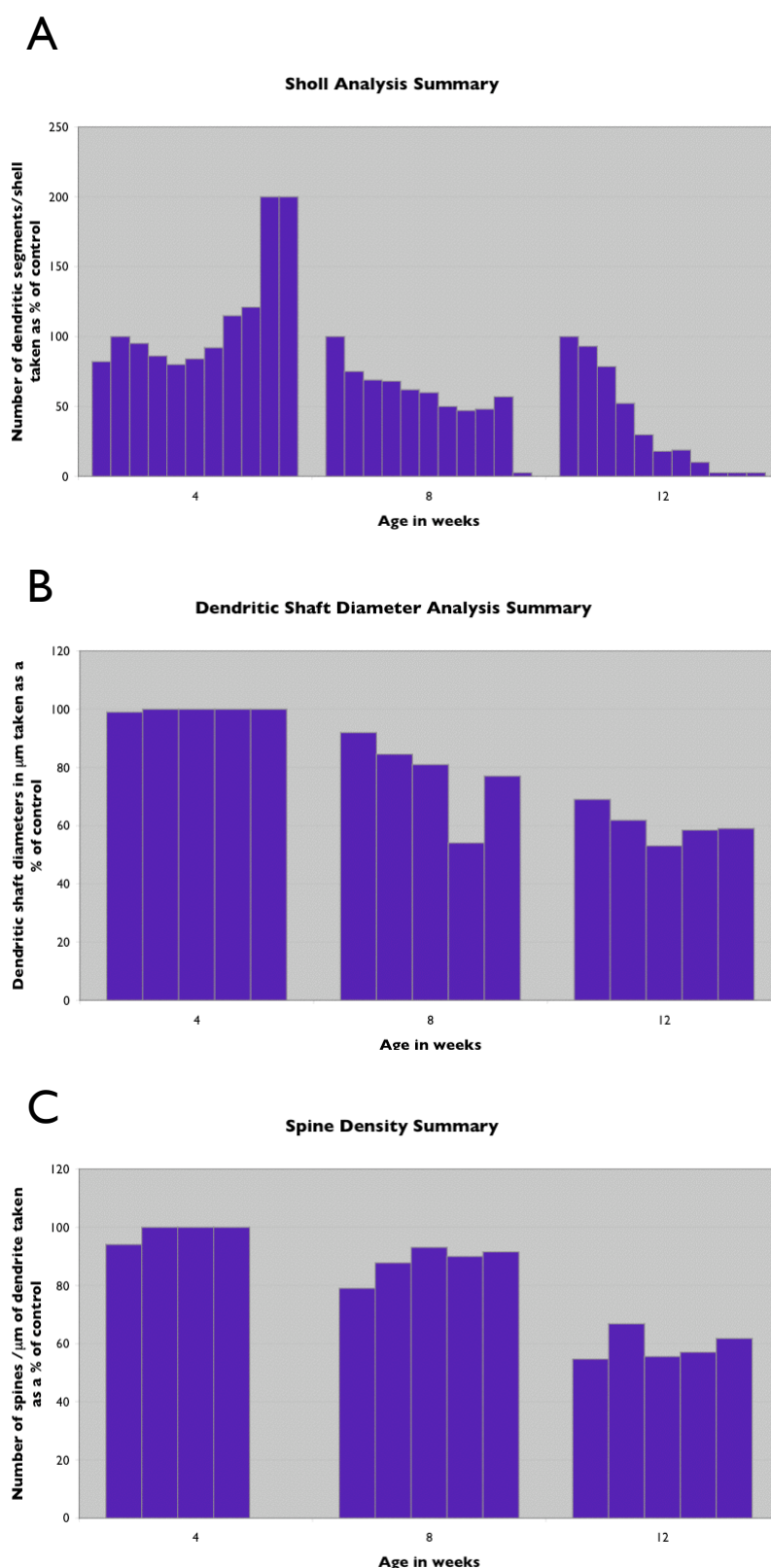


**Figure 6.28:** Summary of the three main parameters of this study the Sholl analysis (A, each bar represents a 20 $\mu\text{m}$  bin, see page 56 and [Figure 2.9](#)), dendritic shaft diameter analysis (B) and spine density analysis (C, each bar represents one branch order, see page 57 and [Figure 2.10](#)) in the R6/2 model which has the most severe pathology. These are all shown as percentage of controls to emphasize any changes.

The most marked changes in these summaries can be seen in the Sholl analysis which suggests that before the pruning event there is a period of sprouting most apparent at the 4 week timepoint at the more distal dendrites. Shaft diameters are pretty well maintained at 4 weeks but then drop at 8 weeks becoming more pronounced at 12 weeks of age, with a similar effect seen in the spine density analysis. The following page shows all the results for dendritic shaft diameters and spine density analyses in [Figures 6.29 & 6.30](#) as a comparison.

### Dendritic shaft diameters of medium spiny neurones in all the HD models studied

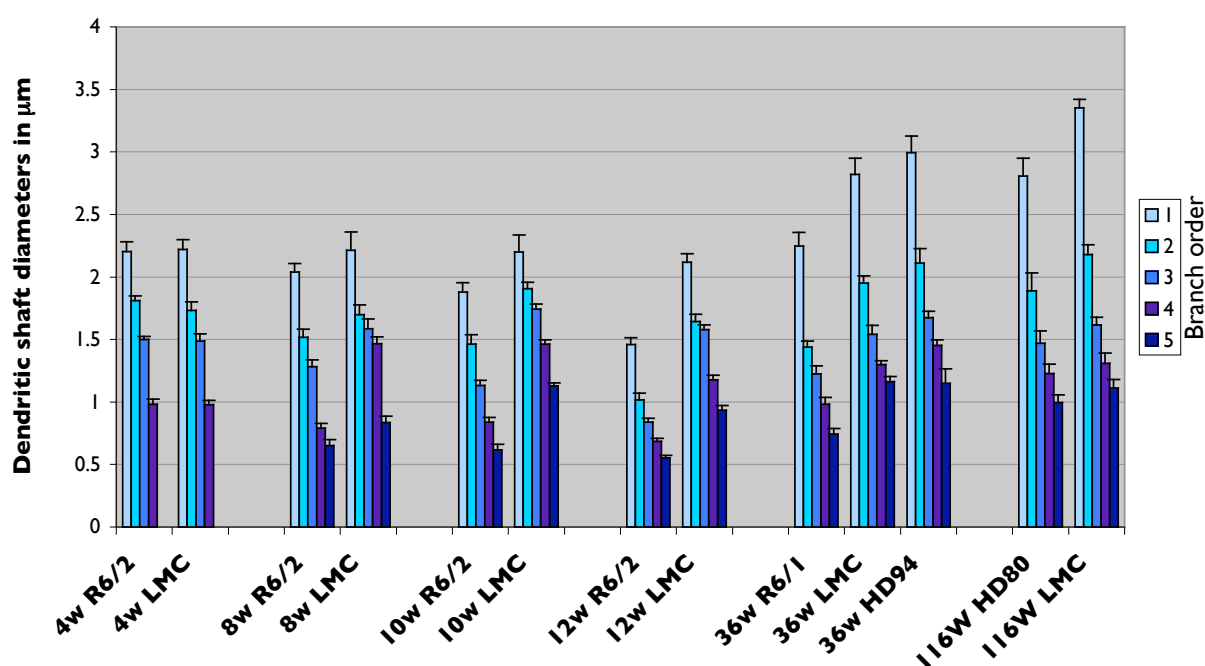
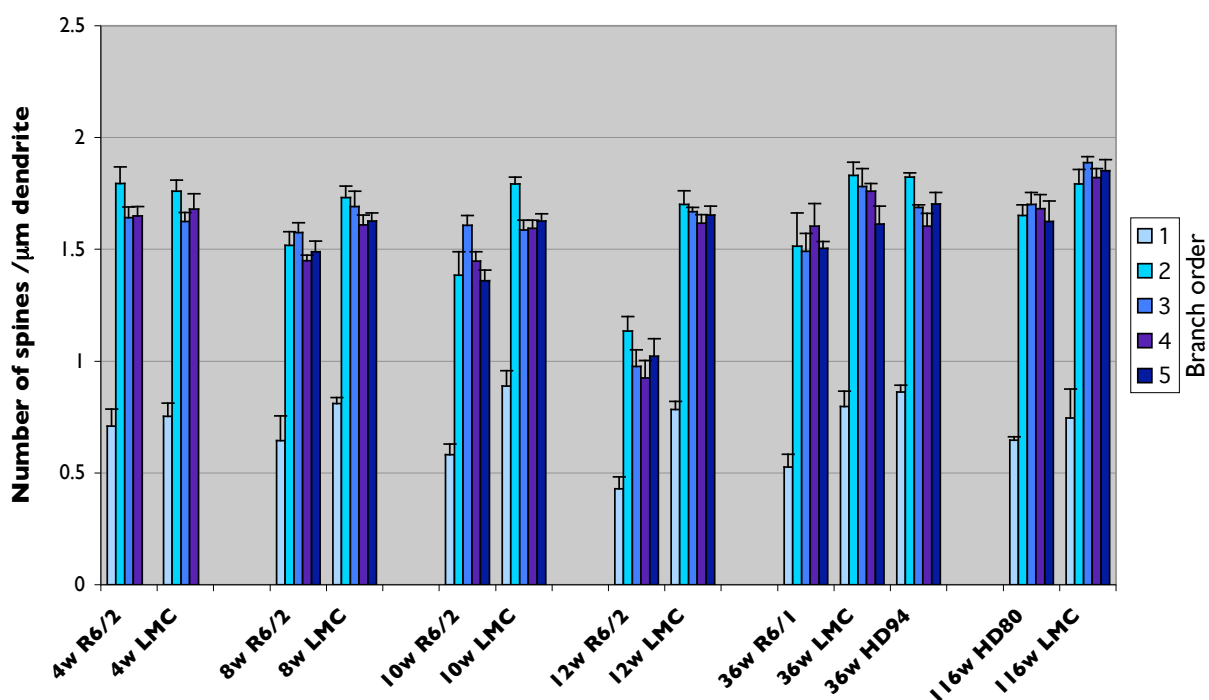


**Figure 6.29:** Graph above shows dendritic shaft diameters in all the models investigated in this study. The numbers in the legend refer to the branch orders of the dendritic arbour.

**Figure 6.30:** Graph below shows the spine density analysis in all the models investigated in this study. The numbers in the legend refer to the branch orders of the dendritic arbour.

### Spine density analysis



The gracile appearance of the dendrites appears also to be a marked pathology as it is apparent in some of the human material which must remain the ultimate benchmark. The dendritic shaft diameters do appear to all be affected in the R6 and to a lesser extent in the HD80 models, once again the HD94 model appears not to be affected in this parameter as can be seen clearly in *Figure 6.29* on the previous page. The pruning and thinning effects in tandem would serve to restrict greatly the surface area of the dendrite on which it is able to accommodate synaptic communication with other neurons.

As would be expected in some cases a severely compromised dendritic arbour and component dendrites the spine density is dramatically reduced in the R6/2 model. Again this effect is seen in a milder version in the R6/1 and subtle form in the HD80 model with the HD94 model remaining pretty unaffected. Where the ultimate pathology may lie would be the spine morphologies which have been handled as a simple analysis in this study but perhaps some of the newer methods of investigating dendritic spines may find out more. The HD94 model does appear to have more gracile looking dendritic spines which have a less defined head and shaft components when compared to LMCs of the same age seen in *Figure 6.19*, perhaps this may be the reason for the reported symptoms in this model (Yamamoto *et al.* 2000). However apart from this subtle pathology very little pathology information has been found in this model which can be taken in context with human HD pathology and those of the other murine models also examined in this study, very little correlates with other findings and is able to contribute to the overall findings which is most disappointing.

On the whole however it can be said that this study has confirmed that HD pathology in murine models at least does have dendritic sprouting followed by pruning and a general decrease in dendritic shaft diameters and spine densities all of which serve to sever communication abilities of the medium spiny neuron. Other affected populations were found in the R6/2 model but these require further thorough investigations to appreciate fully their place in the disease pathology.